Meteorol. Z. (Contrib. Atm. Sci.), PrePub DOI 10.1127/metz/2022/1109

Coastal impacts on offshore wind farms – a review focussing on the German Bight area

Johannes Schulz-Stellenfleth[1*], Stefan Emeis[3], Martin Dörenkämper[4], Jens Bange[5], Beatriz Cañadillas[2,6], Thomas Neumann[6], Jörge Schneemann[7], Ines Weber[5], Kjell zum Berge[5], Andreas Platis[5], Bughsin' Djath[1], Julia Gottschall[4], Lukas Vollmer[4], Thomas Rausch[2], Mares Barekzai[3], Johannes Hammel[2], Gerald Steinfeld[7] and Astrid Lampert[2]

[1]Helmholtz-Zentrum Hereon, Institute of Coastal Systems – Analysis and Modeling, 21502 Geesthacht, Germany
[2]Technische Universität Braunschweig, Institute of Flight Guidance, 38108 Braunschweig, Germany
[3]Karlsruhe Institute of Technology (KIT), Institute of Meteorology and Climate Research (IMK-IFU), 82467 Garmisch-Partenkirchen, Germany
[4]Fraunhofer Institute for Wind Energy Systems IWES, 26129 Oldenburg, Germany
[5]University of Tübingen, ZAG, Environmental Physics, 72076 Tübingen, Germany
[6]UL DEWI – UL International GmbH, 26382 Wilhelmshaven, Germany
[7]ForWind, Institute of Physics, Carl von Ossietzky University Oldenburg, Küpkersweg 70, 26129 Oldenburg, Germany

(Manuscript received August 28, 2021; in revised form February 22, 2022; accepted February 24, 2022)

Abstract

The atmospheric boundary layer experiences multiple changes in coastal regions, especially with wind directions from land towards the sea, where the wind speed usually increases due to the smaller roughness of the ocean surface. These effects are of particular relevance for offshore wind energy utilization; they are summarized under the term coastal effects. This paper provides an overview of coastal effects and their potential impact on the operating conditions of offshore wind farms with a focus on the German Bight. Common numerical and experimental tools to study coastal effects and developing internal boundary layers (IBL) are introduced, and a review on the current state of research is given. The German Bight is an interesting example to illustrate impacts of coastal effects on offshore wind energy, because of the large number of wind turbines with a coastal distance of 100 km or less. Phenomena related to the stability of the boundary layer, like low level jets, are discussed. Spatial variations of vertical heat fluxes in the coastal zone related to variable water depths or Wadden Sea areas are analysed. The study illustrates that due to the increasing size of offshore wind farms, horizontal wind speed gradients caused by coastal effects can lead to significant wind variations within a single farm.

Research topics which still need further attention are discussed in the framework of the rapidly developing wind energy sector with increasing wind turbine hub heights and rotor diameters as well as growing wind farm sizes. One example is the interaction of coastal effects with offshore wind farm wakes. The necessity to consider a large spectrum of spatial and temporal scales to understand and describe coastal effects is highlighted. We summarize modelling and observation tools, which are suitable for the investigation and prediction of the boundary layer dynamics in coastal areas. Existing applications and results are described based on several examples with collocated observation and model results obtained in the X-Wakes project. The study puts particular focus on the large potential provided by the combination of different measurements and modelling techniques and gives recommendations for future developments of integrated approaches including the formulation of priorities.

Keywords: Coastal Effects, Offshore Wind Farm, Atmospheric Boundary Layer, Coastal Observing System, Coastal Modelling System, Low Level Jet

1 Introduction

Offshore wind energy is contributing a significant share in the electricity supply in Germany and worldwide. By the end of 2019, about 1,500 turbines with a combined capacity of 7.4 GW were in operation at the German coast, making the country Europe's second-largest offshore operator following the United Kingdom (WindEurope, 2020). With future planned installed capacities of 30 GW by 2030, 40 GW by 2035 and 70 GW by 2045 the current German government has three long-term goals for offshore wind farm expansion in their coalition agreement (SPD, Bündnis 90/Die Grünen, FDP, 2021). According to the European Union (EU) Strategy on Offshore Renewable Energy, the installed offshore wind capacity in Europe will grow

*Corresponding author: johannes.schulz-stellenfleth@hereon.de

by a factor of five from 12 GW today to 60 GW by 2030. The Global Wind Energy Council (GWEC) Market Intelligence forecasts that by 2030, more than 205 GW of new offshore wind capacity will be added globally, including at least 6.2 GW of floating offshore wind power (Lee et al., 2020a).

The rapid growth of the offshore wind energy sector is a challenge for various research disciplines, which are required to optimise the transition of the energy system. Apart from engineering aspects, this development has an impact on atmospheric, oceanic, biological, chemical as well as societal components and can only be treated in a strongly interdisciplinary approach. This study concentrates on one specific atmosphere physics aspect, which is due to the fact that most offshore wind farms (OWFs) are so far installed in relative proximity to the coastline (see Figure 1a). This is done because the costs for foundations grow with water depth and the costs for the electrical grid increase with distance from the coast. Figure 1b shows the distribution of distances of offshore wind turbines in the German Bight to the coast with respect to different wind directions. For each wind direction sector of 15° and range interval of 30 km the number of turbines is counted, for which the first land point in the given wind direction has a distance to the turbine falling into the specified range.

The plot represents the situation of 2020 and shows that for a significant number of wind turbines the distance to land is 50 km to 200 km for a directional sector of at least 180°. As discussed in the following, the atmospheric conditions at offshore wind farm locations can be significantly influenced by the presence of nearby land.

There are two main reasons why the offshore wind technology has become an attractive option. Firstly, the wind speed over sea is usually significantly higher compared to the wind conditions over land due to the smoother surface. Secondly, as a consequence of the smoother water surface and lower buoyancy fluxes, atmospheric conditions offshore are characterised by smaller turbulence intensities compared to land (Türk and Emeis, 2010), which reduces fatigue loading on offshore structures (Frandsen and Thomsen, 1997).

At least for time scales shorter than the diurnal cycle the atmospheric boundary layer (ABL) over homogeneous ocean or land surfaces is close to an equilibrium with a balance between surface friction, large-scale pressure gradients, and the Coriolis force (Stull, 1988). However, in coastal areas, where most of the existing and planned offshore wind farms are located, complex transition processes between the land and ocean boundary layer take place (Stull, 1988; Emeis, 2018). This phenomenon is of particular relevance for offshore wind directions (in this text offshore wind directions refer to air masses coming from land and going towards the sea), where an internal boundary layer (IBL) forms downstream of the coast line (Garratt, 1990). Three-dimensional (3D) dynamics of the atmosphere in this transition zone are complicated and a challenge for flow assessment and forecast models for different reasons. Firstly, there are uncertainties concerning the required boundary information. For example, it was demonstrated in Hahmann et al. (2020), that wind speed profiles can have a high sensitivity with respect to the specified surface roughness and Wever (2012) showed that there are in fact considerable uncertainties with respect to trends in surface roughness, e.g. related to changing land use. The roughness of the sea surface is complicated by the dependence on wind speed and ocean waves, which are impacted by various parameters like fetch length, water depth or ocean currents (He et al., 2019) and there is still debate about optimal parameterizations (Golbazi and Archer, 2019). Secondly, the formation of the IBL is strongly conditioned by the 3D dynamics of turbulence, and not only horizontal advection (Garratt and Ryan, 1989; Vickers et al., 2001), which is still a challenge for atmospheric models as well (Yang et al., 2019). Thirdly, the stability of the ABL is affected by the sea surface temperature (SST) in the transition region (Garratt and Ryan, 1989; Vickers et al., 2001). SSTs can show significant variations on a spatial scale of a few kilometres often related to variable water depths (Katsaros et al., 1983; Grayek et al., 2011), which are still difficult to capture accurately by either satellite observations or numerical ocean model simulation.

An illustration of the surface temperature variations that can occur within a shallow near-coastal zone is given in Figure 2. Three sea surface temperature transects were acquired by an airborne infrared sensor (Lampert et al., 2020) north of the Jade Bay (see Figure 1a) on 24 July 2021 around 08:00 (green dashed), 13:00 (red dashed) and 17:00 UTC (blue dashed). Isolines of the water depths are superimposed in Figure 2a. The respective measurements between the points A and B are given in Figure 2b. One can see that there is a temperature drop of about one degree between shallow and deeper water along the transects of about 20 km length. In addition, the water along all transects is heating up by about 3 to 4 degree within 9 hours of this summer day. It was shown in previous studies, e.g., Sweeney et al. (2014), that temperature changes of that order of magnitude can have very relevant impacts on the ABL dynamics in the land/sea transition zone.

The treatment of various tasks in the offshore wind energy sector can be optimised by considering coastal effects, e.g.:

- planning (e.g. optimal siting and farm layout) of offshore wind farms requires reliable long-term statistics on wind and wave conditions
- building and operational phases of offshore wind farms require short-term forecasts as well as longer-term statistics on appropriate weather conditions
- maintenance work and the scheduling of back-up power plants keeping the electrical grid in operation require shorter-term forecasts (3–10 hours)

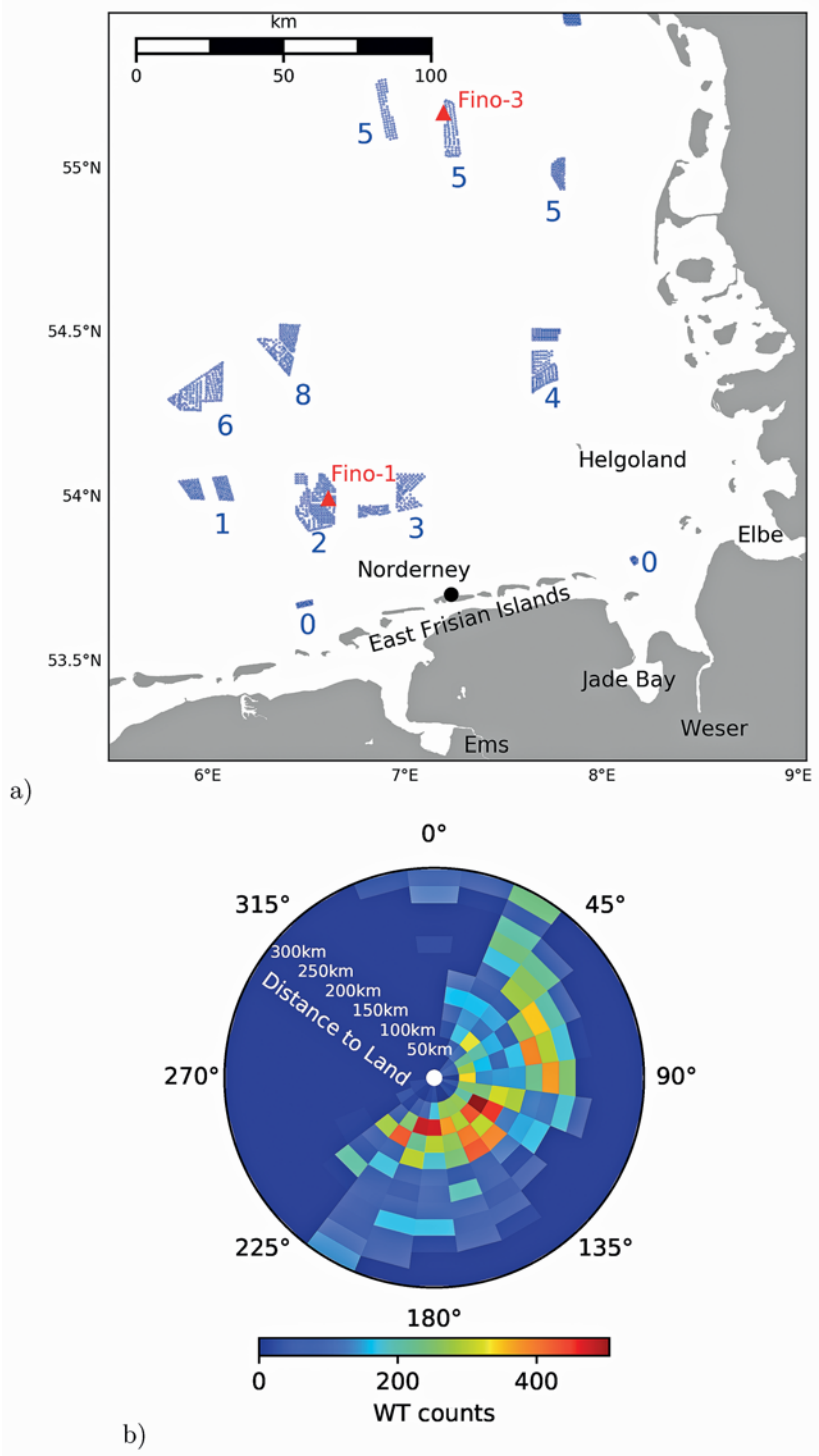

Figure 1: a) Overview map of the German Bight with some geographic locations used in the text and the positions of offshore wind turbines installed by 2020. The blue numbers refer to windpark clusters (BSH, 2019). b) Distribution of upstream distances to the coast for wind turbines in the German Bight in 25 km bins with respect to different wind directions. The plot represents the situation of the year 2020 with 1637 installed offshore wind turbines. WT counts is the number of wind turbines for a specific wind direction sector and a specific distance interval.

- optimization of the trade of produced electricity in the market benefits from shorter-term forecasts (Spyridonidou and Vagiona, 2020; Theuer et al., 2020),
- improvements of the still poor understanding of the interaction of OWF wakes with coastal effects could have an impact on design and operation strategies.

Figure 3 gives an overview of spatial and temporal scales of different coastal effects that will be discussed in the following. In addition, characteristic scales of wind farms were added, in particular wind farm sizes and distances from the coast. One can see that scales of coastal effects definitely have a major overlap with OWF scales. What is not shown is the vertical length

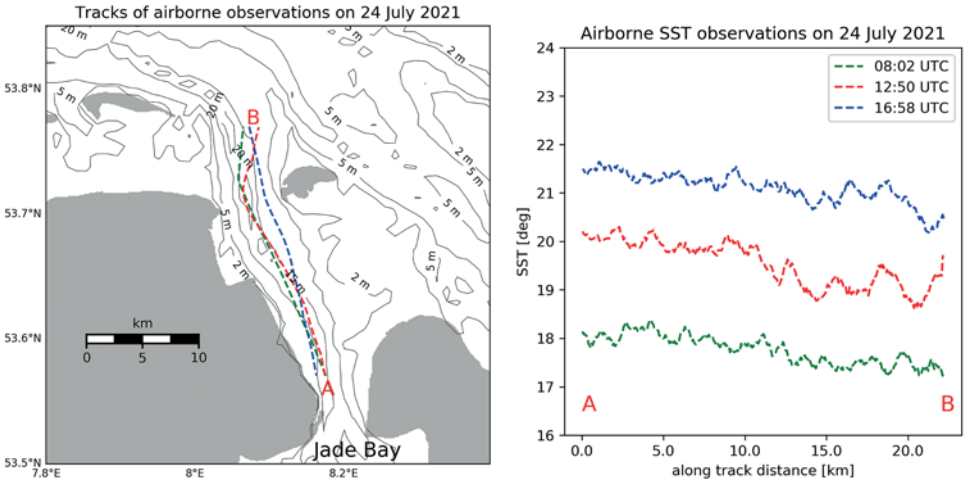

Figure 2: a) Map showing the locations of airborne sea surface temperatures measurements north of the Jade Bay (see Figure 1a) on 24 July 2021. Three tracks measured at different times of the day are shown together with isobaths. b) Corresponding SST measurements between the points A and B.

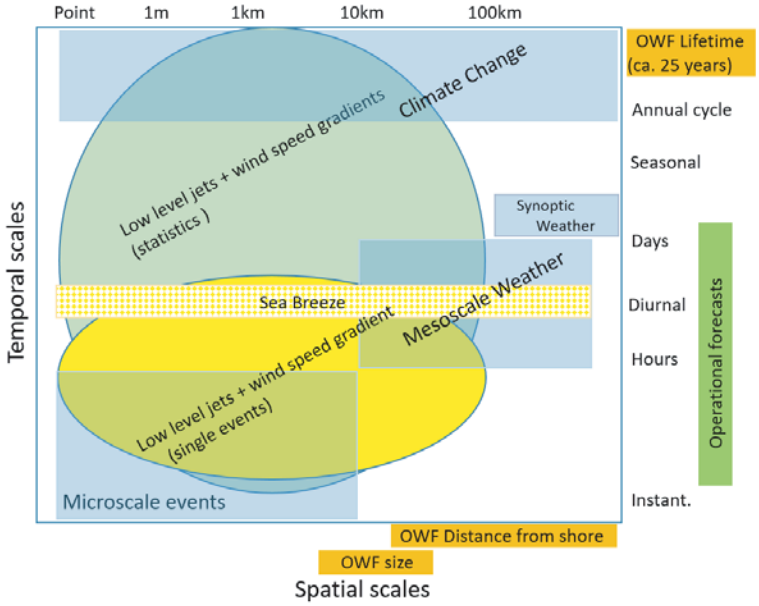

Figure 3: Spatial and temporal scales of different coastal processes related to the offshore wind farm (OWF) sector.

scale where the typical hub height of today's wind turbines is overlapping with relevant vertical scales of coastal effects as well. The sketch also distinguishes between single coastal effect events and long-term trends in the statistics, which can be due to climate change or changes in land use. Whether such trends are relevant within the typical life span of an offshore wind farm of 25 years still needs further investigations. Another interesting fact to consider is that there is also a scale overlap with synoptic weather phenomena, which makes the detection and quantification of coastal effects a particular challenge. This applies also to the time scales that are addressed in operational forecast models. A better representation of coastal effects in these models may lead to improvements, which are relevant for OWF operations, e.g. planning of maintenance on short time scales.

Atmospheric wakes caused by offshore wind farms can be a major issue for the power yield of wind farms downstream (Schneemann et al., 2020; Akhtar et al., 2021). The principle features of such wakes have been investigated in the projects "WIndPArk far field" (WIPAFF) (Emeis et al., 2016; Platis et al., 2018; Platis et al., 2020; Cañadillas et al., 2020; Platis et al., 2021; Platis et al., 2022) and GW-Wakes (Kühn and Schneemann, 2017; Vollmer et al., 2017; Trabucchi et al., 2014) both funded by the German Ministry of Economic Affairs and Energy (BMWi). Evaluation of the performance of wind farm parameterisations in the Weather Research and Forecasting Model (WRF) (Skamarock et al., 2008) have shown that the impact of nearby coasts has to be better considered in such simulations (Siedersleben et al., 2018a). Based on results

achieved in GW-Wakes and WIPAFF, the new BMWK funded project X-Wakes is addressing this issue.

The offshore wind farming sector has very high demands concerning the accuracy of wind forecasts and hindcasts. One important factor is the cubic dependence of the wind power P on wind speed U, i.e. $P \sim U^3$, which amplifies errors in model simulations. For this reason, desirable accuracies for wind speeds are reported to be of the order of 3 % (European Wind Energy Association et al., 2012), which results in relative power errors of approximately 10 %. In the following presentation the challenges associated with coastal effects to reach these high accuracy levels are explained and the tools and approaches to further reduce forecast errors are discussed. It is shown that due to strong spatial wind speed gradients in coastal areas even small model errors, e.g. related to erroneous wind directions or inaccuracies in the boundary layer adjustment process, can have large deteriorating effects on the forecast quality for offshore wind farms. Different factors contributing to model errors in coastal regions are discussed with a particular focus on inaccuracies in the boundary forcing data and insufficient representation of physical processes in the existing numerical models.

The paper is structured as follows: Section 2 gives an overview of the existing literature on coastal effects with a focus on processes, which are of relevance for the offshore wind sector. In Section 3 an introduction is given to the modelling and observation tools which are available today to investigate coastal effects. The potentials and limitations of the tools are discussed based on different examples with co-located measurements and simulations in the German Bight. Section 4 gives a summary of the required research identified in the study. Finally, Section 5 concludes the paper and gives an outlook with a focus on steps required to optimise the integration of observation and modelling systems for an efficient support of the rapidly developing OWF sector in the future.

2 Coastal Effects and their Relevance for OWFs

The following section provides an overview of the existing knowledge on coastal effects and discusses the relevance for the offshore wind farm sector.

2.1 Basic Physical Processes

Coastal effects in the atmosphere are caused by differences between physical properties of land and ocean surfaces. Two dominating factors are to be taken into account:

- ocean surfaces have significantly shorter roughness length scales than common land surfaces;
- ocean water has a significantly larger heat capacity than typical soil.

Typical roughness length scales z_0 for land surfaces are between 10^{-2} m (flat grassland) and 10^{0} m (forests and built-up areas), while common values for the ocean range between 10^{-5} m and 10^{-4} m (Stull, 1988), i.e. there is a difference of at least two orders of magnitude. The heat capacity of water is about $0.004\,\mathrm{J\,kg^{-1}\,K^{-1}}$, whereas land surfaces have typical heat capacity values below $0.001\,\mathrm{J\,kg^{-1}\,K^{-1}}$. In addition, there are significant differences with respect to heat diffusion processes in the upper layers of land and ocean. Depending on turbulence intensities (e.g. related to ocean waves) heat energy can propagate vertically relatively quickly in the upper layers of water compared to soil (Chalikov, 2005). This results in relatively small variations in ocean surface properties (Kawai and Wada, 2007), which is in strong contrast to onshore conditions. Furthermore, there are strong differences concerning the albedo, which is usually lower for the ocean with a typical range between 0.02 and 0.03 for high solar zenith angles with dependencies on various factors like wind speed, water constituents or ocean wave breaking (Li et al., 2006; Sinnett and Feddersen, 2018). The land albedo is usually higher and is strongly influenced by land use and vegetation. For coastal areas influenced by tides, the land mask dividing areas of low and higher albedo cannot be assumed as constant. In the German Bight a Wadden Sea area of about 3500 $\mathrm{km^2}$ size falls dry about twice a day (Becker et al., 1992).

In the following we will give an overview of important coastal effects resulting from the respective land/ocean discontinuity.

2.1.1 Land/Ocean Wind Speed Gradients

As a consequence of the roughness discontinuity, air advected from the land towards the ocean experiences less frictional forces over water leading to an increase in wind speed. At the same time, the relative influence of the Coriolis force grows, which causes a slight clockwise rotation of the wind direction on the northern hemisphere (Emeis et al., 2007). This speed-up effect has been investigated in a number of studies in the past (Taylor, 1969; Taylor, 1970; Mulhearn, 1981; Garratt and Ryan, 1989; Garratt, 1990; Barthelmie and Palutikof, 1996; Lange et al., 2004). For example, Taylor (1969) used a simple 2D model to describe this process assuming a neutral atmosphere and neglecting pressure effects. Simulated profiles for wind speed and normalised shear stresses based on this model are shown in Figure 4 for a wind speed of $10\,\mathrm{m\,s^{-1}}$ at 10 m height over land, a land surface roughness of 3 cm, and an ocean surface roughness of 0.3 mm. It becomes obvious that in this simulation the boundary layer has not reached a new equilibrium even after 60 km. In general, the formation of an IBL is observed, where a relative quick adjustment to the oceanic conditions is taking place near the surface and remainders of the land boundary layer are found at higher altitudes. This so-called residual layer

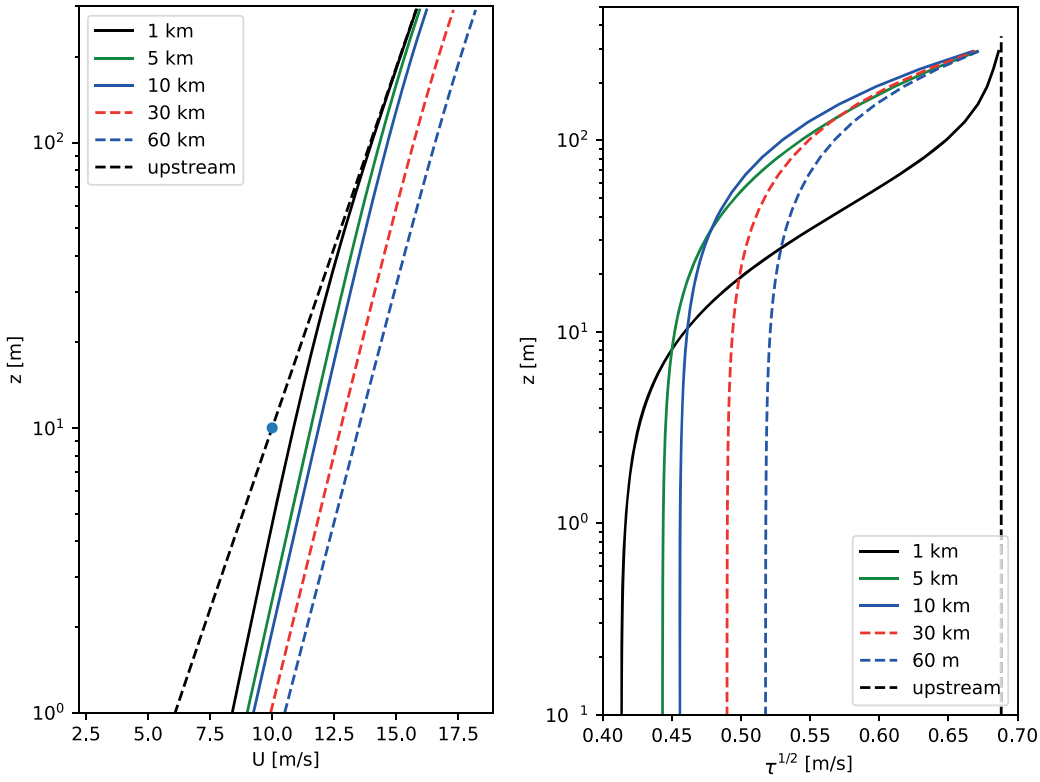

Figure 4: Simulations of wind speed profiles and normalised vertical shear stresses computed with the 2D model presented in Taylor (1969) for different distances to the coastline. A land roughness length of 3 cm, an ocean roughness length of 0.3 mm and neutral conditions were assumed.

(Emeis et al., 2007) is typically characterised by higher turbulence intensities than the air below.

In order to understand the boundary layer adjustment process in more detail, it is necessary to take into account differences with respect to thermodynamic processes within the land and ocean surface layer. Due to the relatively high heat capacity of water, the oceanic temperature response to changes in solar radiation fluxes is much smaller compared to land (Chalikov, 2005). This is reflected by smaller daily and annual temperature variations in the ocean (Kawai and Wada, 2007). As a consequence, significant horizontal gradients can exist in surface temperatures for air masses moving from land towards the ocean. The stabilising effect of cooler water below warmer air advected from land or the respective destabilising effect of cooler air above warmer water has a big impact on the dynamics of the IBL. In general, the IBL adjustment process is accelerated by unstable conditions (Pryor and Barthelmie, 1998; Lange et al., 2004; Barthelmie et al., 2007; Dörenkämper et al., 2015b). For instance, using near-surface satellite derived wind speeds, Djath et al. (2022) showed that horizontal wind fields with thermally unstable stratification adjust towards an equilibrium over shorter distances from the shore than in stable conditions.

The IBL evolution in stable conditions has been investigated in a number of studies (Csanady, 1974; Mulhearn, 1981; Garratt and Ryan, 1989; Smedman et al., 1997). Here, a pronounced IBL forms immediately downstream of the coastline with a warm neutral air mass above. With increasing distance to the coastline the IBL height increases and the stability in the near surface layer tends towards neutral, because the IBL air temperature is adjusting to the colder water temperature. Eventually, a shallow neutral near surface layer forms with remainders of the IBL above. The top of the IBL is typically characterised by an inversion separating the new marine boundary layer and the remainders of the land boundary layer at higher altitudes. Often a low-level jet (LLJ) is forming at this inversion (see Section 2.1.2). In stable conditions it can take several hundred kilometres downstream before the full ABL has reached a new quasi-equilibrium and the inversion has disappeared. For these conditions a simple empirical expression was proposed for the dependence of the IBL height h on the distance to the coast x and the temperature difference $\Delta\theta$ between the sea and the land according to (Mulhearn, 1981; Garratt, 1994)

$$h(x) = 0.015\, u\, (g\Delta\theta/\theta)^{-1/2}\, x^{1/2}\,, \qquad (2.1)$$

where u is wind speed, g is gravitational acceleration, and θ is ocean temperature. More discussion of this issue can be found in Floors et al. (2011); An et al. (2020); Dörenkämper et al. (2015b); Emeis (2018); Shimada et al. (2018); Van Der Laan et al. (2017).

2.1.2 Low Level Jets (LLJs)

Another phenomenon frequently occurring at coastal locations is the low level jet (LLJ). The LLJ is characterized by a wind profile exhibiting a local maximum in wind speed at a particular altitude. Above this altitude wind speed is decreasing again. There are different threshold values for LLJ identification. Frequently, a wind speed difference of at least $2\,\mathrm{m\,s^{-1}}$ and 25 % between the maximum wind speed and the subsequent minimum above is used as criterion (Baas et al., 2006; Lampert et al., 2015; Ziemann et al., 2020). An overview of coastal LLJs on a global scale can be found in Lima et al. (2018). A closer analysis of LLJs and extreme wind shear events at the US east coast was given in Debnath et al. (2021).

Two LLJ formation mechanisms can be distinguished: (1) LLJs which form due to frictional decoupling from the underlying surface, and (2) LLJs due to the thermal contrast between land and sea. The first mechanism can be further split into cases where (1a) the jet forms after the passage of the coastline due to frictional decoupling at the top of an IBL (see Section 2.1.1), and (1b) where jet structures, which have evolved over land due to nocturnal frictional decoupling, are "exported" to offshore areas. The second mechanism can be explained by the definition of the thermal wind (see Wagner et al. (2019) for more details on the different mechanisms). According to this source, LLJs have been observed at 65 % of all days during a campaign over the Southern North Sea from May 2015 to September 2016. Wind LIDAR measurements during a period of one year showed that LLJs occurred during 7 % of the total time at Heligoland, and during 11 % at Norderney (see Figure 1a). Numerous events of stable stratification with LLJs during daytime have been identified here for wind directions from sea to land (8 of 29 daytime LLJ events identified in radiosonde data at Norderney). The stratification for LLJ events during night, measured by radiosonde profiles at Norderney, is mostly neutral or even unstable. An area, which has already been extensively studied with respect to marine LLJs, is the Baltic Sea in Northeastern Europe (e.g. Smedman et al. (1993); Smedman et al. (1995); Smedman et al. (1996)), which is dominated by coastal effects to its full extent. A short climatology of LLJs observed at the Baltic Sea observation platform FINO2 is presented in Dörenkämper et al. (2015b).

LLJs during daytime are mostly expected for wind directions from land to sea, when advection of warm air masses from land to sea, above the colder water surface, results in the formation of an IBL with a temperature inversion at its top (mechanism (1a) above). Nocturnal LLJs can be "imported" LLJs from adjacent land areas if the wind direction is from land to the sea (mechanism (1b) above) or form as a classical LLJ by frictional decoupling (see Dörenkämper et al., 2015b, for an example). Jets due to mechanism (2) can appear at any time of the day.

2.1.3 Horizontal Roll Vortices

In unstable conditions the adjustment of the boundary layer usually takes place over a distance of 10 km or less from the shore line (Dörenkämper et al., 2015a; Dörenkämper, 2015; Dörenkämper et al., 2015b). An interesting phenomenon that was observed under these conditions with both in-situ (Smedman, 1991) and remote sensing techniques (Alpers and Brümmer, 1994) are horizontal roll vortices. These are helical circulation patterns, which extend through the entire mixed boundary layer (Stull, 1988). The vortices are approximately aligned with the mean wind direction and occur in pairs with opposite sense of rotation in the plane perpendicular to the mean flow. In the resulting updraft regions one can typically find the formation of cloud streets. The ratio of the vertical and horizontal dimensions of these structures is roughly 1:3 and a possible misalignment of the vortices with wind direction is stronger in more stable conditions (Stull, 1988).

Explanations for these processes are not straightforward, because different types of instabilities related to inflection points or convection seem to play a role (Etling and Brown, 1993). Furthermore, the roll vortices found in coastal areas often form over land before they are advected over the water (Svensson et al., 2017).

2.1.4 Sea Breeze

There are local wind systems, which do not emerge from large-scale pressure differences, but from regional or local differences in thermal properties of the Earth's surface. These local or regional diurnal wind systems often exhibit a large regularity in climates where radiative cooling and heating is the dominating diurnal feature (Miller et al., 2003). Due to the different thermal inertia of land and sea surfaces, land–sea wind systems can form at the shores of oceans and larger lakes and modify the atmospheric boundary-layer structure. Under clear-sky conditions and low to moderate wind speed, land surfaces become cooler than the adjacent water surface due to long-wave emittance at night and they become warmer than the water surface due to the absorption of short-wave solar irradiance during daytime (Stull, 1988). As a consequence, rising motion occurs over the warmer and sinking motion over the cooler surfaces. A flow from the cool surface towards the warm surface develops near the surface and a return flow emerges in the opposite direction in the upper half of the boundary layer in order to keep the mass balance (Emeis, 2018).

The maximum wind speed in sea breezes can be around $10–11\,\mathrm{m\,s^{-1}}$ at about 100 m height (Atkinson, 1981). Sea breezes originate from a 100–120 km broad coastal zone over the water, detectable from satellite images showing cloud-free conditions in this space (Simpson, 1994). The clouds are dissolved due to the sinking motion in this marine branch of the sea breeze. Fewer observations are available for the nocturnal land breeze,

but it can be assumed that the spatial extent of these winds is comparable to the extent of the sea breeze (Emeis, 2018).

2.1.5 Interaction of Coastal Effects with OWF Wakes

There is some evidence that coastal effects can interact with atmospheric wakes downstream of offshore wind farms, but the relevant mechanisms are still not very well understood so far. The combined effect of increasing wind speeds and reduced turbulence in offshore oriented flow conditions was investigated in Dörenkämper (2015) for a stable boundary layer. The performed Large-Eddy Simulations (LES) for a wind farm 15 km from the coast showed strong wind speed maxima between the turbines. At the same time, the turbulence created by the turbines counteracts a further stabilisation of the boundary layer associated with the cooling of the air by colder water below.

Possible impacts of coastal wind speed gradients on the length of wakes downstream wind farms are also visible in Van Der Laan et al. (2017), although these are not explicitly discussed in this study. The results indicate that, under certain conditions, wakes tend to be shorter if the wind turbines are closer to land, where wind speeds are lower.

2.1.6 Interaction with Synoptic Weather Phenomena

The above mentioned coastline-specific phenomena rarely occur as isolated features under stationary large-scale weather conditions. Usually, the outer conditions such as large-scale horizontal pressure gradients, air mass temperatures and humidity, cloudiness (and linked to this incoming short-wave and outgoing long-wave radiation) change with the emerging, moving and dissipating synoptic-scale weather phenomena. Especially approaching and passing cold fronts can bring severe and abrupt changes to the conditions invoking the above described phenomena. For example, Wagner et al. (2019) describe the interaction between the various LLJ mechanisms with frontal wind maxima. Nearly constant large-scale weather conditions for several days can be expected in temperate latitudes only during blocking situations (Woollings et al., 2018).

2.1.7 Phenomena related to Land Inhomogeneity

The coastline in the German Bight has, like most coastlines, a quite irregular shape characterised by a variety of islands, bays and river entrances. This heterogeneity in the coastline geometry leads to variations in the fetch, i.e., the downstream distance from shore for a certain offshore wind direction. Figure 5 depicts these fetch lengths for a wind direction of $\Phi = 150°$. One can see that there are significant fetch variations due to coastline irregularities. In combination with the wind acceleration effect described in Section 2.1.1 this can result

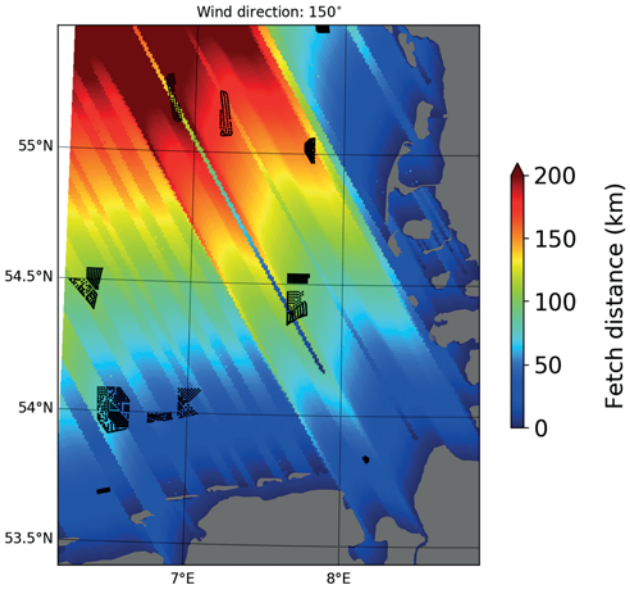

Figure 5: Fetch distances in the German Bight for a wind direction of $\Phi = 150°$.

in larger horizontal wind speed changes perpendicular to the wind directions.

In addition, the topography in the German Bight is quite variable as well. For example, larger parts of most barrier islands are covered with sand dunes. These dunes and the local wind field present a complex interacting system. In the application of offshore wind energy, mostly the effect of the dunes on the local wind field that is advected towards potential wind farms is of interest.

Many ocean coastlines are accompanied by tidal flats, which are flooded roughly twice a day and fall dry in between. This leads to strong variations in surface roughness of about two orders of magnitude (from roughly 0.1 mm to roughly 1 cm) and in thermal inertia properties, which governs the vertical heat fluxes. The difference between high tide and low tide can shift the effective coastline by many kilometres and thus shift the line where the IBL formation starts during offshore winds. Also the sea breeze systems discussed in Section 2.1.4 can be shifted by this effect considerably. A numerical study with the mesocale model WRF, which is discussed in more detail in Section 3.1.1, showing these effects for one of the largest tidal flats in the world in South Korea was performed by An et al. (2020).

2.2 Relevance of Coastal Effects for OWFs

The coastal effects described above are of relevance for offshore wind farms in different ways. As already explained in the context of Figure 3, the spatial and temporal scales of coastal effects and OWFs show a strong overlap leading to often complex and non-linear interactions. This means that these phenomena should be taken into account in the planning, construction and operation phase of an OWF.

For example, the horizontal wind speed gradients associated with coastal effects are of obvious relevance for OWFs, because significant wind speed gradients in the IBL, especially at hub height of the wind turbines can directly affect the wind farm production (Barthelmie et al., 2007). The dimension of most installations has grown so big, that significant wind variations within one wind farm can not only be caused by shadowing effects, but also by coast related gradients in the background wind field. The situation in the German Bight is particularly interesting because the L-shaped coastline leads to limited fetch conditions (i.e., relatively small upstream distances to the coast) for both easterly and southerly winds (see Figure 1). In the Baltic Sea, where plans for significant expansions of offshore wind farming exist as well (European Commission, 2020), such conditions are found for almost all wind directions.

The IBL dynamics is also strongly connected to turbulence intensities experienced by offshore wind farms (Foreman and Emeis, 2012; Foreman et al., 2017). Here, the question is not only whether the boundary layer is stable or unstable, but also where the rotor blades are located with respect to the IBL, i.e., detailed information about the IBL structure is required. The location of the temperature inversion with respect to the wind turbine height results in either cooling or warming of the air within the wakes (Siedersleben et al., 2018b). The vertical structure of the IBL will also be of growing relevance with the increase of rotor diameters in the future, because wind shear in the incoming wind profile across the rotor disc can be a significant factor in the fatigue loading (Micallef and Sant, 2018).

The wind speed variations perpendicular to the wind direction discussed in Section 2.1.7 can lead to significant power variations within a wind farm with strong dependencies on the flow direction.

Wind speed gradients are also important for oceanic processes. Of particular interest for the wind farm sector are ocean waves, which are influenced by a complex interplay of wind direction, bathymetry and internal processes (Bärfuss et al., 2020), because they are of relevance for ship operations, which are typically limited to a significant wave height below 2 m (Halvorsen-Weare et al., 2013), and for fatigue loading on turbine structures (Bhattacharya, 2014). The IBL transition adds some complexity to the theoretical description of ocean wave growth, which is already challenging in its basic form.

During LLJs, profiles of wind speed and wind direction strongly deviate from the logarithmic profile. In many cases, wind is only measured at ground or at a specific altitude, and a power law or logarithmic extrapolation of the wind profile is used to estimate the wind speed at higher altitudes (Justus and Mikhail, 1976). In the presence of coastal effects these simplifications are usually not feasible any longer.

As wind variations caused by horizontal roll vortices are taking place on spatial scales, which are close to characteristic length scales of a wind farm (e.g. rotor diameter hub height, wake width), these processes play an important role in offshore windfarming. For example, it was shown that ABLs can have an impact on the shape and orientation of wakes downstream of OWFs (Dörenkämper et al., 2015b).

3 Analysis Tools for Coastal Effects

In this section an overview is given of different tools, which are relevant in the context of coastal effects on OWFs. Each subsection contains basic technical information, a summary of existing applications in the offshore wind sector as well as a short discussion of ongoing and future developments. In the final subsection the complementarity of the different tools is analysed and discussed with consideration of different research and operational applications.

3.1 Numerical Modelling

3.1.1 Mesoscale Models

Mesoscale atmospheric models like the Weather Research and Forecasting Model (WRF) presented in Skamarock et al. (2019) yield a comprehensive description of the atmosphere and are generally applied with resolutions larger than several kilometers. Therefore, large spatial domains can be covered that connect the wind field at the wind farm with the upwind coast line. The results of the model simulations are used for large scale wind resource assessment studies (Al-Yahyai et al., 2010; Gryning et al., 2014; Rybchuk et al., 2021). A comprehensive assessment of the wind resource over Europe is given by the New European Wind Atlas (NEWA) described in Hahmann et al. (2020) and Dörenkämper et al. (2020).

Mesoscale models are composed of a dynamical core, which solves the Navier-Stokes equation using several scale dependent parameterizations. The parameterizations approximate numerically expensive and physically complex processes like the solar and thermal radiation fluxes, the coupling of the atmosphere to the Earth surface, the turbulent mixing within the lower atmosphere, unresolved deep and shallow convective clouds and the processes including water droplets and ice crystals. Especially, wind farms are parameterized as elevated momentum sinks across the rotor area (Fitch et al., 2012; Volker et al., 2015). An open research question is whether to explicitly include a term for the creation of turbulent kinetic energy (TKE) or if the introduced wind shear will develop the correct TKE independently. These approximations are manifold, not generally valid and introduce uncertainty. Therefore, atmospheric observations which are often limited to a small part of the atmosphere are used to validate the model setup and assess the model error. Siedersleben et al. (2018a) validated the spatial dimensions of the wake

introduced by the wind farm parametrization of Fitch et al. (2012) for the German Bight. The study confirms the results of Lee and Lundquist (2017) that the upwind conditions introduce larger uncertainties than the different wind farm parametrizations themselves. The simulations, however, show poor agreement with observations when the wind is directed from land and the coast line to the wind farm. Furthermore, a horizontal resolution smaller than 5 km is proposed to capture the effects of the wind farm parametrization. This leads to the general issue of limited computational resources, which can be solved by nesting models with increasing spatial and temporal resolution, thereby providing the boundary conditions for the nested models, which must be interpolated to the higher resolution. The boundary conditions for the outer most domain are taken from reanalysis datasets like ERA5 (Hersbach et al., 2020). However, interpolating the data at the model boundaries to the nested model's grid introduces errors that will be advected into the domain and negatively impact the quality of the forecast. Additional simplifying assumptions are often made concerning the roughness length of the ocean surface, where usually the Charnock relation (Charnock, 1955) is used to quantify the influence of sea state. The respective neglection of wave age is so far believed to have a relatively small impact on wind resource estimation (Jørgensen et al., 2005).

A promising development are parametrizations that bridge the gap between mesoscale and higher-resolution Large Eddy Simulations (LES) which are called gray-zone parametrizations. At horizontal resolutions smaller than only a few kilometer the mesoscale assumptions for the treatment of turbulence and convection are not valid anymore. Therefore, new scale-aware turbulence parametrizations are proposed, for example by Zhang et al. (2018), that resolve turbulence in 3 dimensions and could be used instead of the one-dimensional boundary layer schemes. The manifold challenges that arise from coupling the meso and LES scale are presented in Haupt et al. (2019) within the context of wind energy. Finally, the land-sea transition and the changes due to the diurnal cycle are still a challenge for mesoscale models. The diurnal cycle is not only dependent on the change of the radiation itself and the heating of the surface, but also the incident inflow and fetch that can lead to induced stratification at the coastal transition. Thus, a correct representation of the diurnal cycle at coastal sites depends on many parameters, such as sea surface temperature, time-evolving land-sea mask in tidal areas, land surface temperature, wind speed and direction (Sweeney et al., 2014). All of those can in principle be modelled with the mesoscale modelling approach, but a significant improvement can be achieved depending on what model boundary conditions and physics are selected. Interesting research is presented in Lee et al. (2016); Lee et al. (2020b) on the impact of tidal wetlands and the corresponding changes in latent and sensible heat fluxes, which are reduced by inundation during daytime.

3.1.2 Microscale Models

Due to their simplifying assumptions in the turbulence parameterisation, the performance of mesoscale models is usually less satisfactory in close vicinity to the coast than over the open ocean (Yang et al., 2019). LES models aim at resolving the bulk of turbulence in a planetary boundary-layer flow explicitly. The resolution of these models is in the inertial range of atmospheric microscale turbulence. This allows for the application of sub-grid parameterizations that aim at taking the impact of the non-resolved turbulence on the resolved turbulence into account. Due to its ability to resolve the bulk of the turbulence explicitly, LES can help to gain insights into the complex turbulence processes in the coastal marine atmospheric boundary-layer (CMBL).

A pioneer study in which LES was used to investigate an offshore flow was presented by Skyllingstad et al. (2005). These authors studied the evolution of a CMBL with an offshore flow transporting warm air over cool water. Due to the high computational resources required for the LES it was not possible to use a stationary model domain with geographically fixed locations of the inflow and outflow boundaries. Instead a Lagrangian approach was applied: the model domain was assumed to be translated with the geostrophic wind. Instead by imposing horizontally heterogenous surface boundary conditions to describe the heterogeneity at the coast, the surface boundary conditions were changed in time in order to mimic a flow crossing the coastline. Some basic results of this study will be discussed in Chapter 4.

A recent pair of studies in which results from LES with a similar Lagrangian approach as in Skyllingstad et al. (2005) were reported can be found is formed by Jiang et al. (2020) and Jiang and Wang (2021). The focus of Jiang et al. (2020) was on the convective internal boundary layer (CIBL) that forms due to the advection of air that is initially situated above a cool and rough land surface towards a smoother and warmer sea surface. Despite using similar idealizations in the LES setup as Skyllingstad et al. (2005), Jiang et al. (2020) found a good agreement of their LES results with field observations from the CASPER-EAST field campaign (Wang et al., 2018). According to the LES consistency with Monin-Obukhov similarity theory is reached only after 8 km downstream from the coast. Further upstream the surface wind speed and stress increase rapidly. Even at 75 km downstream of the coast the CIBL had not yet reached a state of equilibrium. In Jiang and Wang (2021) the development of a stable internal boundary layer with distance from the coast is investigated. For that purpose the advection of air that is initially situated above a warm and rough land surface towards a cool and smooth sea surface is simulated. According to the LES the CMBL can be divided into three zones for this case. In the zone closest to the shoreline advection of turbulence from the land plays a significant role. In the zone farthest away from the coast Monin-Obukhov similarity

theory was found to be applicable throughout the constant flux layer.

Another LES study refering to the CASPER-EAST campaign was presented by Yang et al. (2019). Here, a stationary, i.e. geographically fixed model domain was used. Moreover, the complex coastal topography is accounted for by making use of an immersed boundary method. Due to the high computational cost that results from the high resolution required to represent the complex topography of the coastline in the model only the flow conditions within the first 1.75 km downstream of the coastal transition could be simulated. With only 250 m the extension of the model domain in the vertical direction was severely limited. Both onshore and offshore flows were simulated and impacts of the coastal transition on turbulence fluxes were analyzed.

A number of LES studies have dealt with the simulation of sea breezes. While Antonelli and Rotunno (2007) used a very idealized setup with an initially resting atmosphere, a recent study aimed at making use of a coupling of the LES to mesoscale simulations in order to study the fine-scale characteristics of sea breeze fronts for specific situations (Chen et al., 2019).

A first LES study in which the impact of the coastal transition on the flow conditions felt by an offshore wind farm is investigated was presented by Dörenkämper et al. (2015b). As in Skyllingstad et al. (2005) the coastal transition was mimicked by a change of the surface conditions with time instead of by applying a geographically fixed model domain with horizontally heterogenous surface conditions.

The advancements in high performance computing clusters has enabled the application of LES for the simulation of coastal flows for research purposes in the last twenty years. So far, specific situations have been studied with LES only. Systematic sensitivity studies are still lacking and only few LES have been done with realistic representations of the topography at the shoreline so far.

3.1.3 Engineering Models

Engineering models, or commonly referred to as wind farm models (e.g. Openwind (Openwind, 2020), Windfarmer (DNV-GL, 2013), Flappy (Schmidt et al., 2020)), are used in offshore wind resource and energy assessments, and for wind turbine layout optimization as part of feasibility studies. They typically rely on wind flow data provided by dedicated external models and model atmospheric physics only as far as wakes and other wind farm effects are concerned. Therefore, they do not require expensive computation time. To account for wind turbine wake effects they rely on analytical wake models with different degree of complexity implemented in the model (Jensen, 1983; Frandsen, 1992; Ainslie, 1988; Bastankhah and Porté-Agel, 2014). Some engineering models also provide a module for the formation of the IBL triggered by large offshore wind farms, which significantly lowers the observed wind speeds inside the farm below the levels calculated from the direct wake models alone (Brower and Robinson, 2009; DNV-GL, 2013). As pointed out in Cañadillas et al. (2020), these boundary-layer models treat the wind farm as an area of increased roughness depending on the actual wind farm geometry. The calculated energy yield inside an offshore wind farm thus depends on the interplay and the parametrization of both the direct wake model and the IBL model. It is worth to mention that these models are usually applied under the assumption of a neutral atmospheric layer and the blocking effect (Porté-Agel et al., 2020) of wind farms has recently started to be considered. Effects of non-neutral stratification (but no horizontal inhomogeneity) have been considered in the analytical model EFFWAKE (Emeis, 2010; Emeis, 2018; Emeis, 2022).

Additionally, the background wind field required as input is commonly based on measured wind data (masts, radiosondes, etc.) in combination with simulated data, e.g. from numerical weather prediction models, computational fluid dynamics (CFD), or simplified models like e.g. WindMap (Beaucage et al., 2009) or WasP (Troen and Petersen, 1989). The topographical discontinuities are provided to the model through sea/land maps (elevation data), coastline and roughness maps.

Engineering or industry models should reliably describe the wind speed profiles over water, including the influence of the surface roughness (which determines the drag exerted by the surface on the atmosphere) length and atmospheric stability (Jørgensen et al., 2005). Surface roughness variations are so far not explicitly taken into account for wind resource assessments as they are both considered to be small (Jørgensen et al., 2005) and partly already included in the wind flow modelling. For simplicity, a constant value of 0.0002 to 0.001 m is commonly used for surface roughness in microscale models like WAsP (z_0 = 0.0002 m) and WindMap (z_0 = 0.001 m).

So far, scarce work has been done on the effect of tidal amplitude on wind speed profiles, which indicates that tidal range does not affect mean offshore wind resource estimates (Jørgensen et al., 2005). Tidal effects are normally not considered in flow models, but as pointed out in Barthelmie (2001) for coastal areas where a moderate to large tidal range exposes tidal flats, assuming that these are always flooded will result in a non-conservative estimate in the models because of the modified surface roughness. Additionally, inhomogeneities in the coastline are expected to cause discontinuities in the inflow approaching an offshore wind farm located near shore when the air is flowing from land to sea. Therefore, wind models that feed into wind farm models must be able to capture all these complex effects. To this end, mesoscale atmospheric models that capture effects down to about 1 km are frequently coupled to microscale models (from very simple models such as WindMap to very complex models such as LES) to decrease the horizontal resolution down to some 50 m or even less. The actual model setup always depends

on the site conditions and the required level of model detail.

In addition, there are various models for load assessments including simplified approaches based on surrogate techniques (e.g. Dimitrov et al., 2018). An overview of these models is beyond the scope of this paper.

3.2 In-Situ Measurements

In-situ measurements can be taken from fixed platforms as well as from manned or unmanned aircrafts. In both cases the measurement sensor is in direct contact with the observed quantity.

3.2.1 Aircraft

In-situ measurements of meteorological parameters can be performed by research aircraft, equipped with a sensor system specialized for meteorological measurements. This has been done with the twin-engine turboprop-powered research aircraft Dornier 128-6 with call sign D-IBUF in the projects WIPAFF (Bärfuss et al., 2019; Lampert et al., 2020) and X-Wakes, and further for different kinds of meteorological research, in particular for investigations of processes in the ABL. Sensors for measuring temperature, humidity, wind speed and wind direction are contained in the nose boom (Corsmeier et al., 2001; Lampert et al., 2020). The measuring rate of 100 Hz with a ground speed of about 65 m s^{-1} results in a spatial resolution of the data of higher than 1 m. The aircraft is capable of performing research flights especially at very low altitudes (e.g. down to 60 m for constant altitude flight legs at the wind farms, and down to 15 m for short time periods during profile measurements), provided that a special permission has been granted for the specific campaign. All important measured and calculated meteorological parameters (wind speed, wind direction, turbulent kinetic energy, eddy dissipation rate, temperature, potential temperature, humidity and surface temperature) can be displayed online with time series and vertical profiles. This enables the onboard scientist to adapt the flight pattern during the mission if necessary, based on the measured parameters. Examples of aircraft data will be presented in Section 3.4.2.

3.2.2 Unmanned Aircraft Systems (UAS)

With fixed wing unmanned aircraft systems (UAS) it is possible to perform measurements analogous to the manned aircraft measurements presented previously, but typically on smaller horizontal scales. UAS can be deployed where manned aircraft systems are limited especially at very low altitudes (e.g. 30 m above surface), very close to wind turbines (e.g. less than one rotor diameter (Mauz et al., 2019)), and in restricted areas such as nature reserves upon permission. Small UAS with wingspans of a few metres and especially using a pusher configuration achieve very high spatial resolutions even into the sub-metre range and hence allow for the investigation of turbulence and effects at scales smaller than the resolution of standard remote sensing instruments and most manned research aircraft.

For measuring coastal effects, the UAS system MASC-3 (Multipurpose Airborne Sensor Carrier Mk 3) developed at the Eberhard-Karls University of Tübingen was deployed (Rautenberg et al., 2019b). These are fixed wing aircraft with 4 m wing span, carrying a meteorological payload of up to 1.5 kg. The sensor payload consists of a five hole probe (Wildmann et al., 2014b; Rautenberg et al., 2019a), a fine-wire platinum resistance thermometer (Wildmann et al., 2013), a hygrometer (Wildmann et al., 2014a; Mauz et al., 2020), and an inertial navigation system (INS) including GNSS. This enables high resolution measurements of the 3D-wind vector, temperature and water vapor. All data are sampled at 100 Hz leading to a post-Nyquist resolution of up to 30 Hz. Combined with a cruising airspeed of 18.5 m s^{-1} this allows measurement of fast variations of thermodynamic quantities on a 1 m scale and hence the calculation of turbulence parameters such as the TKE and turbulent-flux calculation also in very stable thermal stratification. The flight endurance in offshore conditions is approximately 1.5 hours. The UAS is controlled by an autopilot system, flying predefined flight patterns that are highly accurate and reproducible.

At the time of writing, such UAS observations were mainly realized within the visual line of sight (VLOS) of an operator, limiting the operation radius to few kilometers, but sufficient in many cases since the horizontal scales to be covered are only at the lower end of meso-scale modeling or on that of a single wind farm. Beyond visual line of sight (BVLOS) operations will allow for distances up to tens of kilometers. Currently, the required technology in order to meet the legal requirements is under development and testing. We will discuss examples of UAS data in the context of the case study presented in Section 3.4.3.

3.2.3 Meteorological Towers at Land and Sea

The installation of offshore in-situ meteorological towers to collect the desired wind information in the nearshore regions is associated with a high investment, regulatory constraints, and a large effort in the permitting process. For this reason, offshore meteorological towers are still quite sparse (Archer et al., 2014). The FINO1 and FINO3 meteorological towers (see Figure 1a) are a unique measurement source of publicly available in-situ meteorological and oceanographic (metocean) data in the German Bight. FINO1 is already operating since 2003, to our knowledge delivering the longest continuous offshore time series for wind energy worldwide. FINO3 is in operation since 2009 (Leiding et al., 2012). There are some private met masts (e.g., OWP Nordsee Ost (NSO)), the data of which is however not public. In addition, atmospheric profile information is available from the FINO2 platform at the German Baltic Sea coast.

While the original task of these meteorological towers is to observe the environmental conditions near the planned offshore wind areas, they are still in a region where coastal influence is existent. For the investigation of coastal effects, they provide reference data for the almost fully developed offshore boundary layer. They are the only source of long-term data based on high frequency ultrasonic anemometers and they deliver in-situ temperature and humidity profiles, including SST measurements. A growing challenge in the interpretation of FINO1 and FINO3 data is the impact of the increasing number of surrounding wind turbines on the measurements.

3.3 Remote Sensing

Remote sensing devices for wind measurements open up the possibility to measure wind speeds at locations far from the measurement system. This allows for wind field monitoring from the coast, from offshore platforms, or from different moving systems.

3.3.1 LIDAR

In recent years, remote sensing systems like wind LIDAR (Light Detection And Ranging, also Lidar or LiDAR) and particularly Doppler wind LIDAR has been proven to have a high reliability for remote wind measurements (Emeis et al., 2007; Hasager et al., 2013; Peña et al., 2013; Clifton et al., 2018). A single wind LIDAR is able to measure wind speed components in the LIDAR's laser beam direction. To calculate the horizontal wind speed and direction from this measured radial (or Line of Sight (LoS)) wind speed components, several techniques, such as Velocity Azimuth Display (VAD), Doppler Beam Swinging (DBS) or integrating Velocity Azimuth Process (iVAP) together with the assumption of horizontal homogeneity of the flow are applied (Vasiljević et al., 2016).

In the wind energy context, Doppler wind LIDAR has become a commonly used technology, both as profiling LIDARs (fixed laser beam geometry, looking upwards) and scanning LIDARs (more flexible geometry with adjustable laser beam azimuth and elevation angles). Since both profiling and scanning LIDARs are efficient tools to investigate coastal effects, they are briefly discussed in the following.

Profiling LIDARs were originally introduced as a replacement for meteorological towers in wind energy applications. They come along with the advantage of measuring the wind at different heights simultaneously, reaching maximum altitudes above the LIDAR of typically 250 m up to 1000 m and more for short- and long-range systems, respectively. The achievable LIDAR performance depends on the prevailing atmospheric conditions (cloud coverage, aerosol concentration). In the offshore environment profiling LIDARs are deployed at the coast (Shimada et al., 2020; Shimada et al., 2018), on fixed platforms (Hasager et al., 2013; Peña et al., 2013), integrated in or on top of buoys (Gottschall et al., 2017) or on vessels (Gottschall et al., 2018). The fact that profiling LIDARs can provide measurements of the whole wind profile up to a relevant height makes them very suitable for studying LLJs as one of the most typical coastal effects. Specific LLJ studies making use of wind LIDAR measurements were published for the North Sea (Kalverla et al., 2019; Wagner et al., 2019) and Baltic Sea (Hallgren et al., 2020).

Scanning (long-range) LIDARs can be used to cover larger areas and distances allowing to measure how the wind flow evolves when approaching or moving away from the coast. Instruments are typically operated in Plan Position Indicator (PPI: fixed elevation and varying azimuth angle) or Range Height Indicator (RHI: fixed azimuth and varying elevation angle) mode, or in multi-(dual- or triple-) LIDAR mode (Floors et al., 2016; Cameron et al., 2017). Commercially available compact long range scanning LIDARs nowadays obtain wind speed measurements at horizontal distances up to 14 km within the boundary layer. Therefore, careful LIDAR alignment (Rott et al., 2022) and uncertainty estimation of the measurement geometry is crucial (Schneemann et al., 2021; Cañadillas et al., 2021).

Due to the aforementioned formation of the IBL at the coast, the wind speed is expected to increase with distance from the coastline and to be less pronounced at higher altitudes (Shimada et al., 2020). Therefore, not only the vertical but also the horizontal characterization of the wind is important in near shore areas. Long range scanning LIDARs deployed at the coastline could be a valuable tool to characterize or monitor the near shore wind resource (Simon and Courtney, 2016). Examples of LIDAR measurements will be presented as part of the case studies in Sections 3.4.1, 3.4.2 and 3.4.3.

3.3.2 Ground-based Radar

Ground-based Dual Doppler Radar (DD Radar) as developed by Texas Tech University / Smart Wind Technologies comes along with similar advantages as long-range scanning LIDARs, but with significantly larger range and faster scanning capability. Compared to compact scanning LIDARs current Doppler radar devices are much bigger, which makes the deployment more complex and on some offshore structures not possible. The only near-shore deployment so far was demonstrated in the Beacon project (Nygaard and Newcombe, 2018; Valldecabres et al., 2018), for which a DD Radar system was installed onshore close to the coast measuring offshore. Though the objective of the Beacon project has been to study wind farm wakes around and inside a near-shore wind farm, there is an obvious potential for mapping coastal effects as well.

3.3.3 Airborne Laser Scanner

Today, mainly two kinds of data sets for ocean waves are available to the community: point measurements

recorded on buoys or platforms, and satellite altimeter measurements. In between point and satellite altimeter measurements, there is an observation gap for area-covering measurements with small-scale resolution. During the projects WIPAFF and X-Wakes, airborne measurements were performed in the German Bight with the aim to characterize the modified flow-field downwind of offshore wind farms. In that context, laser scanner measurements were performed by the Dornier128 aircraft operated by TU Braunschweig providing information on the small scale roughness and the elevation of the sea surface. The system appears to be very promising for the analysis of coupling effects between the atmosphere and the ocean, such as the impact of atmospheric wakes on ocean wave evolution (Bärfuss et al., 2021).

3.3.4 Satellite Synthetic Aperture Radar (SAR)

Satellite Synthetic Aperture Radar (SAR) is an active microwave system, which operates independent of weather and daylight conditions. At moderate incidence angles (20°– 45°) the radar return is dominated by Bragg scattering, which means that SAR images provide information on the ocean surface roughness at a scale comparable to the radar wavelength (a few centimetres depending on frequency band). As the small scale surface roughness is strongly linked to the near surface wind, SAR has become an established tool for the measurement of 2D wind fields close to the ocean surface (Lehner et al., 1998; Christiansen and Hasager, 2005; Li and Lehner, 2013; Djath et al., 2018; Djath and Schulz-Stellenfleth, 2019). The spatial resolution of the obtained wind fields is typically of the order of 100 m and the coverage can reach up to several hundred kilometres in both dimensions depending on the SAR operating mode. The principle ability of SAR to resolve flow features on a smaller scale has been demonstrated using concurrent Doppler LIDAR measurements (Schneemann et al., 2015; Ahsbahs et al., 2020). The main limitation of satellite SAR measurements is due to the sun-synchronous orbits of the respective platforms leading to revisit periods of typically a few days depending on constraints defined for the imaging geometry. The measurements are always at two fixed times of the day (e.g. around 5:00 UTC and 17:00 UTC for the Sentinel 1 satellites in the German Bight). SAR data have already been used for the analysis of coastal effects in previous studies (Barthelmie et al., 2007). However, this was so far not done for the German Bight and the analysed data sets were very limited. Recent studies focused on the statistical analysis of the horizontal wind fields with respect to offshore winds in the German Bight (Djath et al., 2022). Apart from that, the studies have shown some discrepancies with in-situ measurements, which still need clarification.

There are a couple of developments in the SAR technology, which are not yet fully exploited and which could be of interest for future studies of coastal effects. For example, polarimetric SAR data can help to distinguish between different scattering mechanisms and to identify dry-fallen Wadden Sea areas. Non-Bragg scattering processes can be caused by wave breaking, i.e. polarimetric SAR data can potentially be used to better understand the structure and roughness properties of the sea surface (Viana et al., 2020). An example of SAR wind measurements will be given in the context of the case study presented in Section 3.4.1.

3.4 Complementarity of Tools

As discussed in Section 2 and illustrated in Figure 3, coastal effects cover a wide range of spatial and temporal scales. As so far no single measurement device is able to cover all these scales and because numerical models are still affected by significant uncertainties in our process understanding, an integrated approach is necessary to obtain a more complete picture of coastal processes. In the following we will discuss the complementarity of some of the tools presented in the previous sections. After some general discussion the added value of combining different tools is illustrated based on three case studies.

Aircraft measurements can cover a large area as well as doing vertical profiles of the atmosphere. This allows to get a picture of the wind field and its variations on different spatial and temporal resolutions, filling the gap between satellite and stationary point measurements. Due to the fast sensors, even small and fast variations (e.g., turbulent kinetic energy) are measured. A measurement flight, depending on the mission, takes up to several hours. This means it is only a snapshot of the current atmospheric situation. The assumption that the atmospheric conditions are stationary during the measurements is not always valid. Measuring the full extent of the wake by the aircraft over such a time span may comprise temporal changes in the atmospheric conditions and if the effect investigated is comparably small (e.g. wind farm blockage effects), natural variations in the wind field, e.g. induced by the coast, can be higher than the effect investigated.

With diurnal variations, and sometimes additionally changing air masses flowing in on the one hand, and the changing position of the aircraft on its flight path during several hours on the other hand, the separation between spatial and temporal variability of the observed weather situation is sometimes not distinctively possible. But if these limitations are considered, aircraft measurements are a valuable contribution to the analysis of coastal effects and complement long term measurements as provided by LIDAR or measurement towers. For measurements very close to the ground or very close to the coast unmanned aircraft systems (UAS) are more suitable due to legal reasons and safety concerns. To reduce the mentioned limitation of only measuring a snapshot of the current atmospheric situation, the use of multiple aircrafts measuring at the same time should be considered.

Satellite data provide large coverage and have potential for the optimisation of numerical mesoscale models because the range of spatial scales is similar. Because of the sparse temporal sampling it is questionable, whether improvements can be achieved using data assimilation methods in an operational mode to improve short term forecasts. However, the low frequency of data acquisitions is less critical for the optimization of uncertain model parameters and the reduction of systematic model errors. This approach, which includes challenging inverse modelling problems, should be investigated more in the future.

Another important aspect is the combination of surface information obtained from satellites with profile information acquired by aircraft, UAV, LIDAR or mast measurements. As explained before, the vertical structure of the ABL can be very complicated in coastal areas and simple extrapolation of surface measurements to hub height is often not feasible. Furthermore, profile information can help in the interpretation of satellite radar data, because simplifying assumptions about the ABL stability are usually made in the respective wind speed retrieval algorithms.

Finally, it is important to mention, that the additional use of supervisory control and data acquisition (SCADA) data, which provide information about the operational status of wind farms, can be crucial for a meaningful interpretation of the measurements discussed above. Access to these data is controlled by industry and usually requires special agreements concerning confidentiality and use restrictions.

3.4.1 Case Study on 14 March 2020

An interesting situation on 14 March 2020, for which co-located satellite SAR and LIDAR measurements as well as WRF simulations are available, is shown in Figure 6. A measurement flight south of the OWF Godewind (see cluster 3 in Figure 1a) was performed earlier, around 11:00 UTC to 15:00 UTC, showing stable conditions in the measurement area. This was a relatively cold day with near surface air temperatures around 7 °C–8 °C and wind coming from the south east. The 2 m air temperatures as provided by the operational model run at the DWD in Figure 6e indicate an increase from the north east towards the south west with temperature differences of around 2 °C across the German Bight. The water temperatures were around 7 °C with only small spatial variations. The air temperature gradient was causing a higher thermal stability in the south/western part of the area as shown in Figure 6f. Around the time of the satellite acquisition at 17:16 UTC a LIDAR located at Norderney (see Figure 6c, d) measured profiles of wind speed and wind direction with a quite pronounced temporal variation. The wind speed profiles in Figure 6c acquired between 16:00 and 18:00 UTC indicate an increase by about 2 m s^{-1} and a stabilisation with increased vertical gradients above 100 m height. As expected, the wind directions show a stronger clockwise rotation with height for the stable situations, because the decoupling from the rough surface makes the Coriolis force more dominant.

The near surface wind speeds estimated with the WRF model (Figure 6a) and derived from Sentinel-1A SAR data (Figure 6b) show overall reasonable agreement. There is a clear downstream wind speed increase from the land towards the sea by roughly 7 m s^{-1} over 200 km. This horizontal wind gradient is shown to follow a power law (Djath et al., 2022). There are bigger differences in the eastern and western part, where the SAR measurements indicate a smaller wind speed gradient than the model. In the SAR data the gradient seems to be stronger in the eastern part, where the stability is lower. As already discussed in Section 2.1.1, the response of the boundary layer to the surface roughness change can be expected to be stronger in unstable situations. In addition, both SAR and WRF show fetch effects, which cause wind variations across stream direction due to the irregular shape of the coastline. This can be observed downstream of the estuaries of the rivers Ems and Weser as well as the Jade Bay (see Figure 1a). The respective fetch lengths for that wind direction are shown in Figure 5.

This example is illustrating a couple of important aspects. Firstly, one can see that due to the big spatial heterogeneities even small inaccuracies in the numerical model, e.g. with respect to wind direction or the ABL adjustment process, can lead to large prediction errors for certain wind parks. Looking at wind park cluster 4 (see Figure 1a) significant differences can be seen between measurement and simulation with regard to both wind speed magnitude (about 20 % error) and spatial variations within the cluster. Secondly, the example demonstrates the fast dynamics of wind profiles at altitudes, which are relevant for OWF operations. Thirdly, the SAR observation show that wind speed gradients can extend way beyond 100 km, i.e., even OWFs far offshore can be affected by this phenomenon.

3.4.2 Case Study on 23 July 2020

Figure 7 shows results from aircraft and LIDAR measurements co-located with WRF simulations on 23 July 2020. For end of July it was a cold, overcast day with some rain showers and wind from south westerly directions. The air temperature above ground measured at the DWD weather station on Norderney at 07:00 UTC was 13 °C–14 °C rising to 21 °C around 10:00 UTC. The SST measured by the aircraft (Figure 7c) was ranging from 15 °C in the north-western part of the measurement area to 17.5 °C in the south-eastern part close to the coast and therefore shallower water. Figure 7d shows the ERA5 SST output that was used within the WRF model. The measurements and simulations are in good agreement with the model slightly overestimating the SST when compared to the measurements. But one has to keep in mind that the measurements were done over a time span of four hours, while the model result is only a snapshot at noon when the air temperature was already

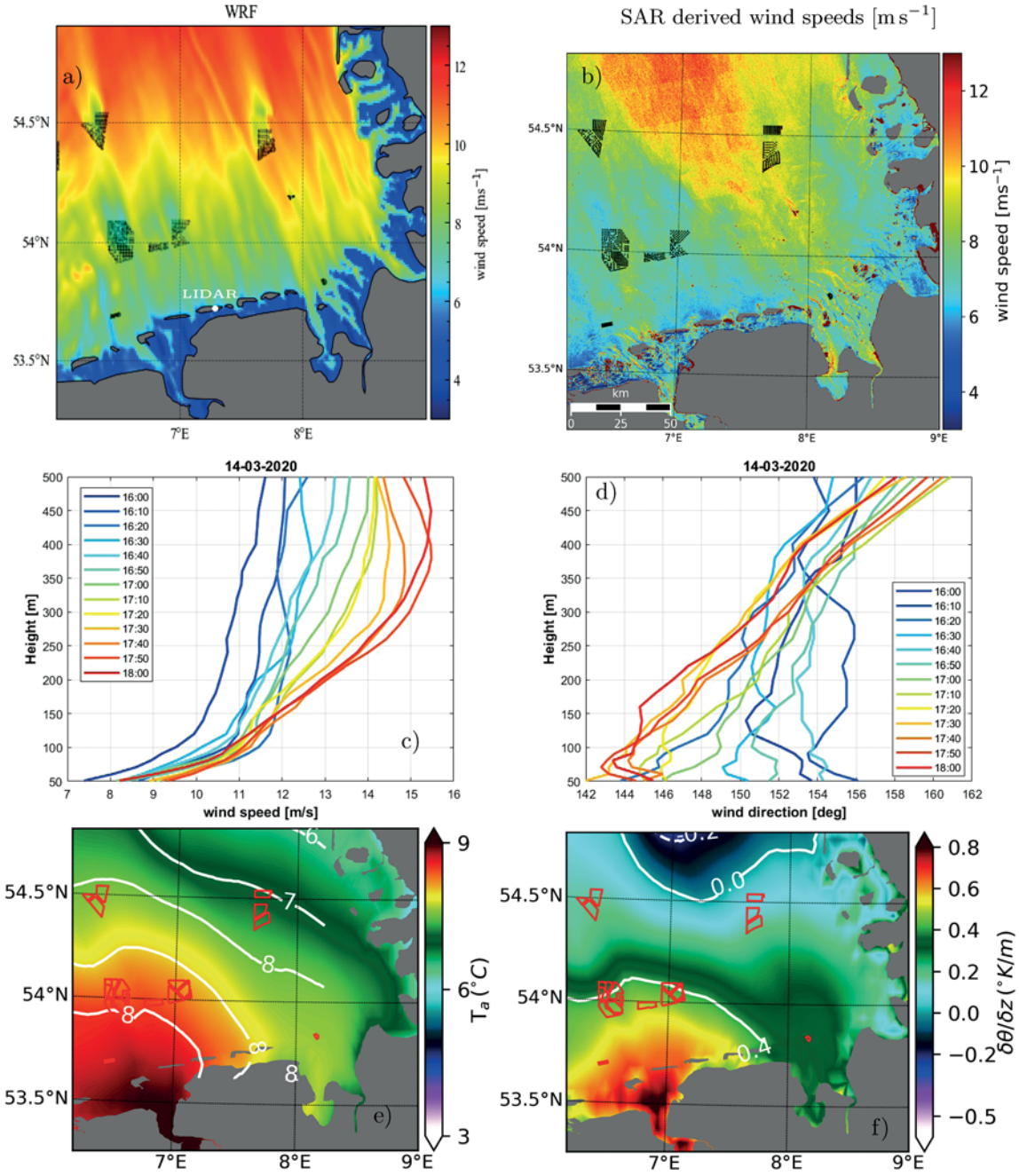

Figure 6: Near surface wind speed from the mesocale model WRF (a) and from the SAR onboard the satellite SENTINEL-1A (b) at 17:16 UTC on 14 March 2020 (Copernicus data (2020)). (c, d) Co-located vertical profiles of wind speeds (c) and wind directions (d) measured by a LIDAR located at the island of Norderney. (e, f) Estimates of 2 m air temperature (e) and thermal stability (f) provided by the operational German weather service model.

peaking at that time. However, the SST gradients in east-west direction of about 2 °C over 50 km indicated by the airborne system are not due to temporal variability, because the aircraft was flying tracks parallel to the coast. This spatial variability of SST is clearly underestimated by the ERA4 data.

Figure 7a shows the mean horizontal wind at hub height (112 m a.m.s.l.) measured by the aircraft. It is visible that the main land mass of North-West Germany and the Netherlands with the Ems estuary has a large impact on the offshore wind field. Over the water body of the Ems Estuary with its much smaller roughness length the wind speed is considerably higher compared to the flow over the coastal regions of North Germany, which is obvious in the higher wind speed measured downstream of this bay. Between 15 km and 45 km distance from the coast low wind speeds between 3 m s^{-1} and 7 m s^{-1} were measured with an exception of a small area at the most western end of the measurement trajectory. Here, the wind speed ranges from 7 m s^{-1} to 10 m s^{-1}. At a distance of around 45 km North of the main land, the wind speed increases with distance to the coast. This in-

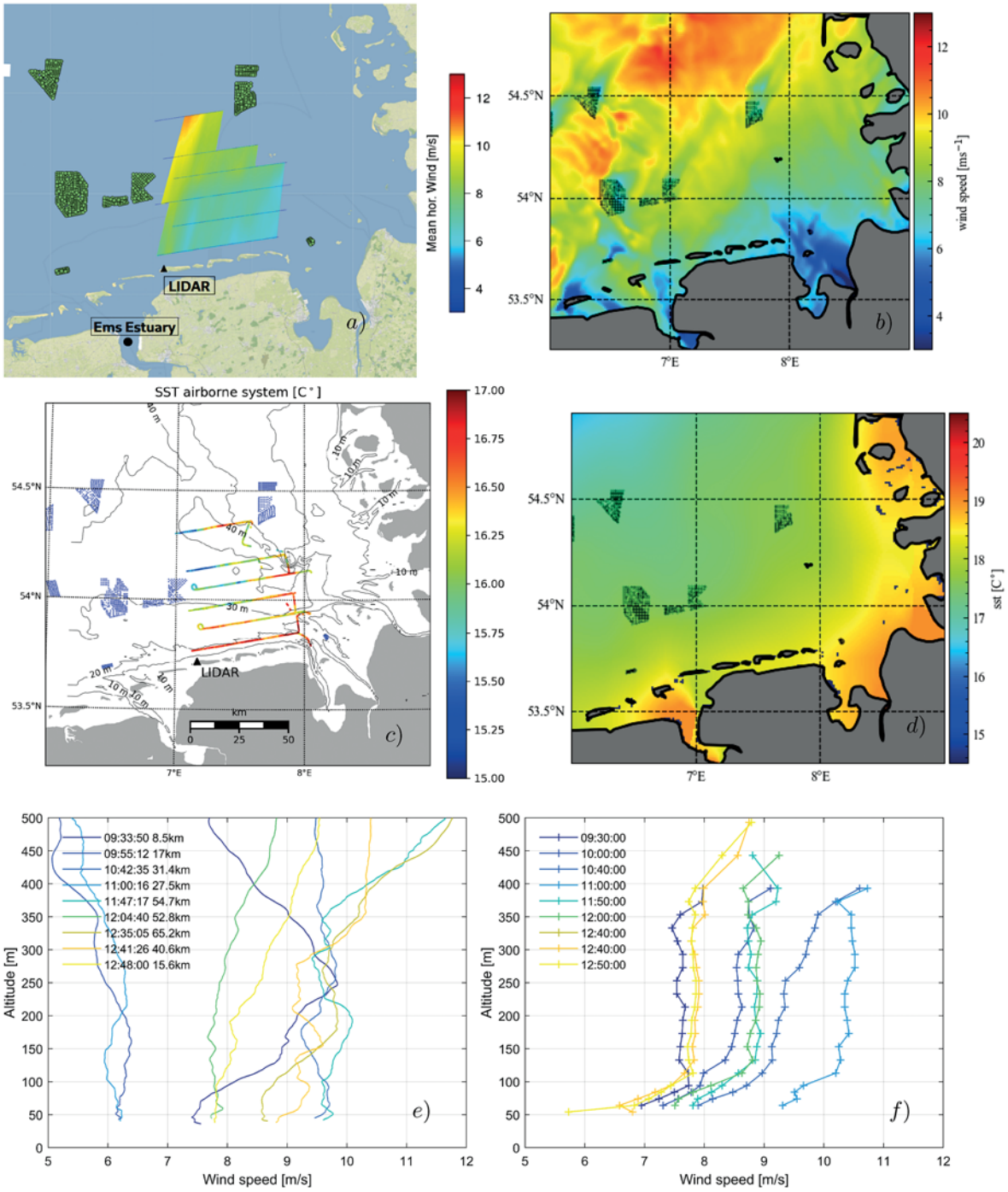

Figure 7: Wind speeds at hub height (100 m–120 m) from aircraft measurements (a) and from the mesoscale model WRF (b) for 23 July 2020 at 12:00 UTC. Sea surface temperature (SST) measured by the aircraft (c) and from the mesocale model WRF (d) for 23 July 2020 at 12:00 UTC. Vertical profiles of the mean horizontal wind speed from aircraft measurements (e) at different locations during the flight and measured simultaneously by a LIDAR located at the island of Norderney (f).

crease in wind speed is again more dominant towards the most western parts of the flight trajectory, reaching nearly 12 m s^{-1}. These higher wind speeds in the most western part of the measured area are also visible in the WRF simulation in Figure 7b. The wind speed close to the coast north of the East Frisian Islands (see Figure 1a) ranges from 4 m s^{-1} to 6 m s^{-1}, while the western area north of the Dollart and further away from the coast shows higher wind speeds above 8 m s^{-1}. The vertical profiling of the wind speed done by the aircraft in Figure 7e and the LIDAR on Norderney in Figure 7f show a similar range of wind speeds between 6 m s^{-1} to 11 m s^{-1} for the lowest 500 m above the sea. Here, we have to consider that the aircraft is moving in time and space. So each of the shown profiles was done at different times during the flight but was as well done at differ-

ent locations. The LIDAR on the other hand measures the diurnal variations while being fixed to one location. We can see the wind speed increasing to nearly 11 m s^{-1} over time until 09:00 UTC and then decreasing to less than 9 m s^{-1} at 11:00 UTC. Due to the aircraft also covering a large area, it is difficult to see the same behavior in the wind speed data in Figure 7e. The two vertical profiles with lower wind speeds around 5–6 m s^{-1} were taken in the most south-eastern area of the flight path, so an area that is very close to the coast and therefore largely impacted by the coastal effect. Very interesting is the vertical profile at 09:33 UTC. It shows a LLJ at 250 m altitude above ground with nearly 10 m s^{-1} wind speed, while only half an hour later the LLJ disappeared. This profile was as well very close to the coast. It is possible the LLJ was still apparent, but not measured by later vertical profiles due to the plane now being further away from the coast line.

This case study shows that a combination of different approaches with different time and length scales to measure and simulate a complex atmospheric phenomenon like the coastal effect has benefits. The rather coarse simulation using WRF gives a good overview of the synoptic situation, while the aircraft measures small scale differences in wind and temperature over a large area and LIDAR at different locations can keep track of the diurnal cycles in wind conditions. Combined these methods are a powerful tool to identify strong gradients in wind conditions on fairly small areas like bays or other irregularities in the coastline and quantify the effect the coast has onto the wind field and therefore on OWFs far away from the coast. The example has also shown that the SST data used as boundary forcing for the model did not contain the spatial variability indicated by the observations. The observed differences have an order magnitude, which was shown to be relevant for the ABL dynamics in coastal areas in previous studies (Sweeney et al., 2014)

3.4.3 Case Study on 30 September 2020

Another interesting situation observed by different measurement systems and simulated by the WRF model occurred on 30 September 2020. On this day UAS flight measurements and LIDAR vertical wind measurements were conducted from the East Frisian Island of Norderney. Technical details for these systems were given in Sections 3.2.2 and 3.3.1. The location of the LIDAR on Norderney as well as the UAS tracks north of the island are depicted in Figure 8a. The wind was coming from southerly directions on that day (about 160°–180°), i.e., the air was coming from land resulting in conditions as described in Section 2.1.1. The UAV flight measurements took place between 12:24 and 13:24 UTC. A continuous vertical ascent up to 600 m was performed followed by a meander pattern at 30 m, 50 m, 80 m and 120 m altitude with three different distances to the shoreline. The length of the measurement legs is 1.2 km and the meridional distances between the measurement legs is approximately 350 m. The measured wind speeds and virtual potential temperatures are shown in Figure 8b and Figure 8c. One can see that the wind was moderate with speeds around 5 m s^{-1}. The wind speed is clearly increasing from about 5 m s^{-1} near the surface to about 7 m s^{-1} at 500 m. There are only small gradients noticeable in the meridional and zonal directions. The WRF simulation of wind speed shown in Figure 8d illustrates that this is not surprising, because the horizontal scale of this gradient is much larger than the area covered by the UAS. The virtual potential temperature shows a near neutral situation below 100 m altitude. Around 100 m altitude a rapid temperature decrease is observed indicating unstable conditions followed by slightly stable stratification further up. The LIDAR wind speed profiles shown in Figure 8e demonstrate considerable temporal variations in the vertical gradients. One can see that the wind speeds between 100 m and 350 m are close to constant at the beginning and the end of the observation period. Within a period of 10 min a significant positive gradient can be observed, which is consistent with a stabilisation within that altitude band already suggested by the UAV temperature measurements. This example is an illustration of the strong dynamics of the boundary layer, which can occur on relatively small spatial and temporal scales due to either local processes or advection from land. Rapid changes of the vertical wind profile were observed on a time scale of 10 minutes and spatial variations of virtual potential temperatures were noticeable on sub-kilometer scale.

4 Required Research

There is still a large number of open questions concerning the understanding and modelling of coastal effects.

The challenges associated with the modelling of the ABL across a land/sea boundary are illustrated in Skyllingstad et al. (2005), where comparisons between a mesoscale and a microscale model showed a deeper boundary layer in the mesoscale model compared to the LES. The profiles of turbulent kinetic energy showed significant differences between the two modeling approaches. The origin of these differences could be traced back to the mixing-length in the turbulence closure scheme used in the mesoscale model. A comparison with data from a measurement campaign showed LES results were closer to the observations, although the strength of turbulence was overpredicted by the LES. Microscale simulations are still limited by available computer resources, but their value for coastal effect studies is obvious and should be exploited more in the future.

Concerning the surface roughness, more work is still required to better estimate roughness length scales for land and the ocean. For land surfaces different forms of usage (e.g. cities, agriculture, forests) as well as vegetation (including annual cycle) are often updated every few years only and more frequently updated datasets

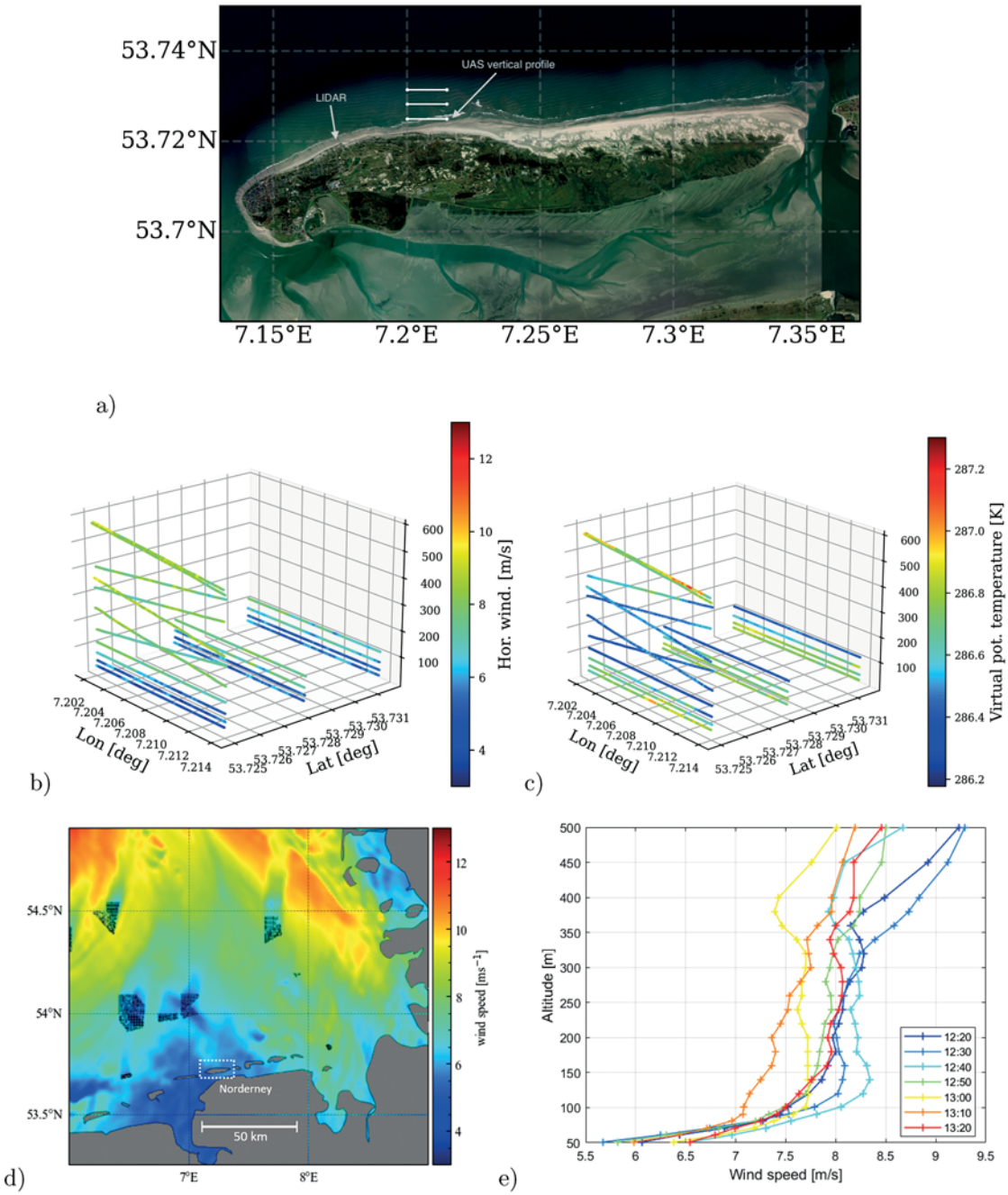

Figure 8: (a) Optical image of the island Noderney with the position of the LIDAR system and the UAS tracks. (b, c) UAS measurements of wind speed (b) and potential temperature (c) on 30 September 2020 around 12:00 UTC. (d) Wind speed map computed with the mesoscale model WRF. (e) Vertical wind speed profiles measured by the LIDAR system on Norderney during the time of the UAS flights.

might be helpful. In case of time-dependent land-use such as in tidal areas this impact should be taken into account. New satellite-based estimation techniques can be used to improve wind resource modelling onshore (e.g. Floors et al., 2021). Offshore, roughness lenghts are mostly estimated by the Charnock relation which was developed for open seas and needs improvements in case of fetch limited conditions which are common in coastal areas. For the ocean the dynamics of wind generated surface waves plays an important role. In case of offshore wind directions these waves are growing in amplitude and length with increasing distance from the coast (Hasselmann et al., 1973; Bärfuss et al., 2021). The interaction of the waves with the ABL during this growth phase is known to be complicated and more work is required to optimise the representation of this process in mesoscale atmospheric models (Wahle et al., 2017).

The estimation of SST in coastal regions is a challenge, because different processes are interacting. First of all, one can observe a strong water depth dependence with faster heating and cooling in shallow water (Becker et al., 1992; Grayek et al., 2011). Secondly, horizontal temperature gradients are advected by mean ocean currents (e.g. due to tides), which contain uncer-

tainties as well (Schulz-Stellenfleth et al., 2021). Finally, the vertical mixing of the water column can have a strong effect on surface temperatures (Becker et al., 1992). As ocean mixing is dependent on many factors (e.g., bed friction, ocean waves, current shear, stability of the water column), there is still significant uncertainty in the estimation of SST (O'Carroll et al., 2019). Improved estimates of near shore SST fields would certainly be beneficial for optimised representations of coastal effects, because these can have a big impact on the evolution of the ABL (Sweeney et al., 2014; Shimada et al., 2015).

The change of surface properties caused by wetting and drying in Wadden Sea areas still needs further investigations both from the modelling and the observations side. Changes with respect to momentum and heat fluxes can be expected and the respective impact on the boundary layer with possible implications for offshore wind farms should be analysed.

There are still a lot of open questions about the interaction of coastal effects with offshore wind farms. The current growth of offshore wind turbine diameters and hub heights requires a better understanding of the wind conditions at higher altitudes above ground that can be significantly impacted by e.g. low-level jets. The impact of coastal effects on wind farm production has only been studied for a low number of wind farms in particular in closer proximity (< 25 km) to the next shoreline.

Concerning LLJs, the frequency of occurrence of the combination of wind directions from sea to land and stable stratification during day should be determined in more detail, using measurements and simulations, in order to better enable the specification of its statistical distribution, its vertical and horizontal extent, and thus the formation mechanism behind. In particular measurements of temperature profiles close to the coast should be improved to derive stability. While vertical profiles of wind speed and wind direction can be measured relatively easily with a wind LIDAR, it is so far not possible to continuously record profiles of temperature, except for meteorological towers, which are rare.

Finally, the possible impact of climate change on coastal effects requires more detailed analysis. For example, it is not clear what consequences water temperature trends in the North Sea (Høyer and Karagali, 2016) will have for the formation and structure of the IBL. Furthermore, there are indications that the statistical distribution of both wind speeds and wind directions will change (Sterl et al., 2015). This may have consequences for the frequency of certain coastal effects as well as their intensity. Additional effects can be expected due to sea level rise, which was observed to be of the order of 1–2 mm/year in the North Sea since 1800 (Wahl et al., 2013) and which may accelerate considerably in the decades to come (Howard et al., 2019). In the long run rising water levels will have an impact on the Wadden Sea areas in the German Bight with consequences for the thermodynamic properties of the land/sea transition zone. Further consequences can be expected for the ocean wave dynamics and the associated roughness properties of the sea surface. A big uncertainty exists with regard to the resulting morphodynamic processes, e.g. whether the Wadden Sea areas will grow in the vertical due to adjusting sediment transport processes.

5 Conclusions and Outlook

An overview was given of the existing knowledge concerning coastal effects, which are relevant for the offshore wind energy sector. The discussion used the German Bight as an example, where a growing number of wind farms is installed in relative proximity to the coast. The presented material is of relevance also for other coastal regions (e.g. USA or Japan), where wind farms are placed even closer to the coast (up to 10 km). It was explained that coastal effects are important in all phases of an OWF's life time and that a large number of atmospheric and oceanic mechanisms have to be considered. One effect of particular interest is the expected wind speed increase with growing distance from the land in situations of offshore wind directions. It was illustrated that a large number of offshore wind turbines is located in areas with significant horizontal wind speed gradients associated with the coastal effect. With the growing size of wind farms, it can be expected that wind speed variations within single wind farms caused by these gradients will become more pronounced. A second important process discussed in more detail is the low-level jet. This phenomenon can lead to very high wind speeds and strong vertical shear in the rotor area and is usually connected to situations with high stability of the boundary layer. This process is an example where the advection of the land boundary layer (e.g., the stable nocturnal boundary layer) towards the sea plays an important role. A second example where this is often the case are atmospheric boundary rolls, which typically form over land in unstable conditions before they are shifted over water. LLJs are however not limited to situations with offshore wind directions and can be triggered by different mechanisms.

A number of scientific challenges were identified that deserve more attention in the future. The most important topics discussed are the following:

- turbulence dynamics in the internal boundary layer is impacted by horizontal variations of vertical heat fluxes in the land/sea transition zone and these should be considered more carefully, in particular in cases with strong spatial variability of sea surface temperatures;
- heat flux variations due to drying and flooding in Wadden Sea areas are not well understood and not well captured by models so far;
- heat flux variations due to water depth variations with quicker cooling and heating of shallow areas should be considered more carefully;

- sea surface roughness variations due to different stages of sea state development are usually not taken into account in numerical models;
- interaction of coastal effects with OWF wakes is not well understood so far, in particular there are open questions with regard to the impact of coastal gradients on wake lengths;
- information on land roughness variations needed as input for numerical models is still sparse, in particular concerning roughness variations due to changing land use or tidal flats;
- more work is required to better understand the interaction of coastal effects with synoptic weather phenomena, e.g., the passage of cold fronts introduces additional complexity;
- coastal effects in the assessment of offshore wind farm energy performance (AEP) using engineering/ industrial models have not been studied in detail so far and model validation using, for example, SCADA data would be very valuable for the wind community as well;
- nearshore measurements are very scarce and, due to the inhomogeneities of the coast, it would be very crucial to have a better combination of in-situ measurements and remote systems, not only to better understand coastal flow but also to validate flow models.

Some of the above challenges have to do with lack of basic process understanding, while others are related to still insufficient spatial resolution of the respective numerical models and forcing data. There are additional very relevant questions, like the impact of climate change on coastal effects, which are beyond the scope of this paper and require more attention in the future.

Available modelling and observation tools were presented and the synergy potential was discussed for different research and operational applications. It was emphasized that the large spectrum of spatial and temporal scales of coastal effects require the combination of different techniques. On the modelling side, mesoscale models can cover the entire relevant coastal area, but require some simplifying assumptions, in particular about the turbulence dynamics. LES models have a more solid foundation in first order physical principles, but are so far limited to relatively small domains due to computational constraints. On the observation side, in-situ data at fixed locations usually provide only limited information on spatial variations, but are still valuable to monitor atmospheric and ocean parameters continuously and with high temporal resolution. On the other side, satellite data can be used to obtain a snapshot view of a particular situation with good spatial resolution, but the sampling frequency is poor and the information usually limited to the atmospheric conditions close to the sea surface. Airborne measurements from manned or unmanned aircraft have a big potential to deliver a comprehensive 3D picture of particular situations with both large coverage and high resolution. Ground or platform based remote sensing devices like scanning LIDAR or RADAR cover smaller areas compared to satellite SAR or aircrafts, but offer the possibility for continuous wind field monitoring over long periods with a good temporal resolution. The following recommendations are given for the further evolution of different tools and in particular for the integration of information from observations and models in the future:

- inverse modelling techniques could be applied to use observations for the optimisation of uncertain model parameters;
- measurement strategies could be developed to monitor coastal effects on longer time scales in order to detect possible trends related to climate change or changing land use;
- coastal effects could be better represented in industrial models used by offshore wind farm developers and operators;
- oceanic and atmospheric observations and models could be better linked to capture important two-way interaction processes, e.g., impacting vertical heat fluxes;
- more analysis is required of stochastic and systematic errors in different modelling and observation tools on spatial and temporal scales relevant for coastal effects;
- observations which are available continuously could be assimilated into numerical models to optimise state estimates for routine applications.

Inverse modelling approaches require four main components: 1) a numerical model, which is able to replicate the main characteristics of the observations, 2) some idea about the origins of the dominating model errors, 3) information about observations errors, and 4) a numerical scheme, which is able to adjust uncertain model parameters such that the agreement between simulated and actual measurements is improved.

Many of the above points are not only important in the context of coastal effects, but in more general terms. In particular, the analysis of interactions between coastal effects and OWF wakes will require an integrated approach based on a variety of tools. With the increasing size of wind farms this topic will grow in importance and strategic planning is required. There is some urgency in this topic because the rapid growth of offshore installations has led to a situation where free stream conditions to be used as a reference are increasingly hard to find.

6 Acknowledgements

The work presented in this study originates from the projects WIPAFF (grant number 0325783) and X-Wakes (03EE3008) both funded by the ministry of economic affairs and climate action (BMWK) based on a decision by the German Bundestag. Computing resources were partly provided by the North-German Supercomputing Alliance. The authors would like to thank the aircraft crew Rolf Hankers, Thomas Feuerle, Mark Bitter and Helmut Schulz.

References

Ahsbahs, T., N.G. Nygaard, A. Newcombe, M. Badger, 2020: Wind Farm Wakes from SAR and Doppler Radar. – Remote Sensing **12**, DOI: 10.3390/rs12030462.

Ainslie, J.F., 1988: Calculating the flowfield in the wake of wind turbines. – Journal of Wind Engineering and Industrial Aerodynamics **27**, 213–224 Publisher: Elsevier.

Akhtar, N., B. Geyer, B. Rockel, P.S. Sommer, C. Schrum, 2021: Accelerating deployment of offshore wind energy alter wind climate and reduce future power generation potentials. Scientific Reports **11**, 1–12.

Al-Yahyai, S., Y. Charabi, A. Gastli, 2010: Review of the use of numerical weather prediction (NWP) models for wind energy assessment. – Renewable and Sustainable Energy Reviews **14**, 3192–3198, DOI: 10.1016/j.rser.2010.07.001.

Alpers, W., B. Brümmer, 1994: Atmospheric boundary layer rolls observed by the synthetic aperture radar aboard the ERS-1 satellite. – Journal of geophysical research **99**, 12613–12621, DOI: 10.1029/94JC00421.

An, H.Y., J.H. Jeong, Y.H. Kang, H. Kim, Y.K. Kim, Z.H. Shon, 2020: Numerical simulations of the impacts of land-cover change in the intertidal zone on local meteorology in western Korea. – Terrestrial, Atmospheric & Oceanic Sciences **31**, 337–349.

Antonelli, M., R. Rotunno, 2007: Large-eddy simulation of the onset of the sea breeze. – Journal of the atmospheric sciences **64**, 4445–4457.

Archer, C.L., B.A. Colle, L. Delle Monache, M.J. Dvorak, J. Lundquist, B.H. Bailey, P. Beaucage, M.J. Churchfield, A.C. Fitch, B. Kosovic, others, 2014: Meteorology for coastal/offshore wind energy in the united states: Recommendations and research needs for the next 10 years. – Bulletin of the American Meteorological Society **95**, 515–519.

Atkinson, B., 1981: Meso-scale Atmospheric Circulations – Academic Press, London, 495.

Baas, A., F. Bosveld, H. Klein Baltink, 2006: Classification of low-level jets at cabauw. – In: 17th Symposium on Boundary Layers and Turbulence.

Barthelmie, R., 2001: Evaluating the impact of wind induced roughness change and tidal range on extrapolation of offshore vertical wind speed profiles. – Wind Energy: An International Journal for Progress and Applications in Wind Power Conversion Technology **4**, 99–105 Publisher: Wiley Online Library.

Barthelmie, R., J. Palutikof, 1996: Coastal wind speed modelling for wind energy applications. – Journal of Wind Engineering and Industrial Aerodynamics **62**, 213–236 Publisher: Elsevier.

Barthelmie, R., J. Badger, S. Pryor, C.B. Hasager, M.B. Christiansen, B. Jørgensen, 2007: Offshore coastal wind speed gradients: Issues for the design and development of large offshore windfarms. – Wind Engineering **31**, 369–382 Publisher: SAGE Publications Sage UK: London, England.

Bastankhah, M., F. Porté-Agel, 2014: A new analytical model for wind-turbine wakes. – Renewable Energy **70**, 116–123.

Beaucage, P., M. Brower, J. Manabianco, 2009: The WindMap microscale model. Technical report, AWS Truewind, LLC Technical Report.

Becker, G., S. Dick, J. Dippner, 1992: Hydrography of the German Bight. – Mar. Ecol. Prog. Ser. **91**, 9–18.

Bhattacharya, S., 2014: Challenges in design of foundations for offshore wind turbines. – Engineering & Technology Reference **1**, 922.

Bärfuss, K., R. Hankers, M. Bitter, T. Feuerle, H. Schulz, T. Rausch, A. Platis, J. Bange, A. Lampert, 2019: In-situ airborne measurements of atmospheric and sea surface parameters related to offshore wind parks in the German Bight. – PANGAEA, DOI: 10.1594/PANGAEA.902845.

Bärfuss, K., B. Djath, A. Lampert, J. Schulz-Stellenfleth, 2020: Airborne lidar measurements of the sea surface properties in the German Bight. – IEEE Transactions on Geoscience and Remote Sensing, DOI: 10.1109/TGRS.2020.3017861.

Bärfuss, K., J. Schulz-Stellenfleth, A. Lampert, 2021: The Impact of Offshore Wind Farms on Sea State Demonstrated by Airborne LiDAR Measurement. – Mar. Sci. Eng. **9**, DOI: 10.3390/jmse9060644.

Brower, M., N. Robinson, 2009: The OpenWind deep-array wake model: development and validation. Technical report, AWS Truepower; Albany, NY, USA.

BSH, 2019: Site Development Plan 2019 for the German North Sea and Baltic Sea, No. BSH-No. 7608. Bundesamt für Seeschifffahrt und Hydrographie (BSH), Hamburg and Rostock, URL: https://www.bsh.de/DE/PUBLIKATIONEN/_Anlagen/Downloads/Offshore/FEP/EN-Flaechenentwicklungsplan2019.pdf?__blob=publicationFile&v=4.

Cameron, L., A. Clerc, S. Feeney, P. Stuart, 2017: Remote Wind Measurements Offshore Using Scanning LiDAR Systems. Technical report, RES Ltd, Kings Langley, United Kingdom.

Cañadillas, B., R. Foreman, V. Barth, S. Siedersleben, A. Lampert, A. Platis, B. Djath, J. Schulz-Stellenfleth, J. Bange, S. Emeis, T. Neumann, 2020: Offshore wind farm wake recovery: Airborne measurements and its representation in engineering models. – Wind Energy 1–17, DOI: 10.1002/we.2484.

Cañadillas, B., M. Beckenbauer, J. Trujillo, M. Dörenkämper, T. Neumann, A. Lampert, 2021: Observation of wind park cluster wakes by a long-range scanning wind lidar and flight measurements. – submitted to Wind Energy Science

Chalikov, D., 2005: Similarity theory and parameterization of mixing in the upper ocean. – Environmental Fluid Mechanics **4**, 385–414.

Charnock, H., 1955: Wind stress on a water surface. – Quarterly Journal of the Royal Meteorological Society **81**, 639–640 Publisher: Wiley Online Library.

Chen, G., H. Iwai, S. Ishii, K. Saito, H. Seko, W. Sha, T. Iwasaki, 2019: Structures of the sea-breeze front in dual-doppler lidar observation and coupled mesoscale-to-les modeling. – Journal of Geophysical Research: Atmospheres **124**, 2397–2413.

Christiansen, M.B., C.B. Hasager, 2005: Wake effects of large offshore wind farms identified from satellite SAR. – Remote Sensing of Environment **98**, 251–268, DOI: 10.1016/j.rse.2005.07.009.

Clifton, A., P. Clive, J. Gottschall, D. Schlipf, E. Simley, L. Simmons, D. Stein, D. Trabucchi, N. Vasiljevic, I. Würth, 2018: IEA Wind Task 32: Wind lidar identifying and mitigating barriers to the adoption of wind lidar. – Remote Sensing **10**, 406, DOI: 10.3390/rs10030406. Publisher: Multidisciplinary Digital Publishing Institute.

Corsmeier, U., R. Hankers, A. Wieser, 2001: Airborne turbulence measurements in the lower troposphere onboard the research aircraft dornier 128-6, d-ibuf. – Meteorol. Z. **10**, 315–329.

Csanady, G., 1974: Equilibrium theory of the planetary boundary layer with an inversion lid. – Boundary-Layer Meteorology **6**, 63–79 Publisher: Springer.

Debnath, M., P. Doubrawa, M. Optis, P. Hawbecker, N. Bodini, 2021: Extreme wind shear events in US offshore wind energy areas and the role of induced stratification. – Wind Energy Science **6**, 1043–1059, DOI: 10.5194/wes-6-1043-2021.

Dimitrov, N., M.C. Kelly, A. Vignaroli, J. Berg, 2018: From wind to loads: wind turbine site-specific load estimation with surrogate models trained on high-fidelity load databases. – Wind Energy Science **3**, 767–790.

Djath, B., J. Schulz-Stellenfleth, 2019: Wind speed deficits downstream offshore wind parks – A new automised estimation technique based on satellite synthetic aperture radar data. – Meteorologische Zeitschrift **28**, 499–515, DOI: 10.1127/metz/2019/0992.

Djath, B., J. Schulz-Stellenfleth, B. Canadillas, 2018: Impact of atmospheric stability on X-band and C-band Synthetic Aperture Radar imagery of offshore windpark wakes. – Journal of sustainable and renewable Energy **10**, DOI: 10.1063/1.5020437.

Djath, B., J. Schulz-Stellenfleth, B. Cañadillas, 2022: Study of coastal effects relevant for offshore wind energy using spaceborne synthetic aperture radar (SAR). – Remote Sensing **14**, DOI: 10.3390/rs14071688.

DNV-GL, 2013: WindFarmer v.5.2 Theory Manual. Technical report, Garrad Hassan and Partners.

Dörenkämper, M., 2015: An investigation of the atmospheric influence on spatial and temporal power fluctuations in offshore wind farms Ph.D. thesis, University of Oldenburg, Oldenburg.

Dörenkämper, M., B. Witha, G. Steinfeld, D. Heinemann, M. Kühn, 2015a: The impact of stable atmospheric boundary layers on wind-turbine wakes within offshore wind farms. – Journal of Wind Engineering and Industrial Aerodynamics **144**, 146–153 Publisher: Elsevier, DOI: 10.1016/j.jweia.2014.12.011.

Dörenkämper, M., M. Optis, A. Monahan, G. Steinfeld, 2015b: On the Offshore Advection of Boundary-Layer Structures and the Influence on Offshore Wind Conditions. – Boundary-Layer Meteorology **155**, 459–482, DOI: 10.1007/s10546-015-0008-x.

Dörenkämper, M., B.T. Olsen, B. Witha, A.N. Hahmann, N.N. Davis, J. Barcons, Y. Ezber, E. García-Bustamante, J.F. González-Rouco, J. Navarro, M. Sastre-Marugán, T. Sīle, W. Trei, M. Žagar, J. Badger, J. Gottschall, J. Sanz Rodrigo, J. Mann, 2020: The making of the new European wind atlas – part 2: Production and evaluation. – Geoscientific Model Development **13**, 5079–5102, DOI: 10.5194/gmd-13-5079-2020.

Emeis, S., 2010: A simple analytical wind park model considering atmospheric stability. – Wind Energy **13**, 459–469.

Emeis, S., 2018: Wind energy meteorology: atmospheric physics for wind power generation, 2nd edition. – Springer International Publishing AG, Cham.

Emeis, S., 2022: Analysis of some major limitations of analytical top-down wind farm models. – Bound.-Layer Meteorol., published online first 24 Janaury 2022, DOI: 10.1007/s10546-021-00684-4.

Emeis, S., M. Harris, R.M. Banta, 2007: Boundary-layer anemometry by optical remote sensing for wind energy applications. – Meteorologische Zeitschrift **16**, 337–347 Publisher: Schweizerbart'sche Verlagsbuchhandlung.

Emeis, S., S. Siedersleben, A. Lampert, A. Platis, J. Bange, B. Djath, J. Schulz-Stellenfleth, T. Neumann, 2016: Exploring the wakes of large offshore wind farms. – Journal of Physics: Conference Series **753**, 092014.

Etling, D., R. Brown, 1993: Roll vortices in the planetary boundary layer: A review. – Boundary-Layer Meteorology **65**, 215–248.

European Commission, 2020: Baltic Sea Offshore Wind Joint Declaration of Intent. url: https://ec.europa.eu/energy/sites/ener/files/signature_version_baltic_sea_offshore_wind.pdf.

European Wind Energy Association, others, 2012: Wind energy-the facts: a guide to the technology, economics and future of wind power – Routledge, London, 488 pages.

Fitch, A.C., J.B. Olson, J.K. Lundquist, J. Dudhia, A.K. Gupta, J. Michalakes, I. Barstad, 2012: Local and mesoscale impacts of wind farms as parameterized in a mesoscale NWP model. – Monthly Weather Review **140**, 3017–3038, DOI: 10.1175/MWR-D-11-00352.1.

Floors, R., S.E. Gryning, A. Peña, E. Batchvarova, 2011: Analysis of diabatic flow modification in the internal boundary layer. – Meteorologische Zeitschrift **20**, 649–659.

Floors, R., A. Peña, G. Lea, N. Vasiljević, E. Simon, M. Courtney, 2016: The RUNE experiment – A database of remote-sensing observations of near-shore winds. – Remote Sensing **8**, 884 Publisher: Multidisciplinary Digital Publishing Institute.

Floors, R., M. Badger, I. Troen, K. Grogan, F.-H. Permien, 2021: Satellite-based estimation of roughness lengths and displacement heights for wind resource modelling. – Wind Energy Science Discussions 2021, 1–34, DOI: 10.5194/wes-2021-28.

Foreman, R., B. Cañadillas, T. Neumann, S. Emeis, 2017: Measurements of heat and humidity fluxes in the wake of offshore wind turbines. – Journal of Renewable and Sustainable Energy **9**, 053304.

Foreman, R.J., S. Emeis, 2012: Enhancing the Simulation of Turbulent Kinetic Energy in the Marine Atmospheric Boundary Layer. – In: Progress in Turbulence and Wind Energy IV, Springer, 163–166.

Frandsen, S., 1992: On the wind speed reduction in the center of large clusters of wind turbines. – Journal of Wind Engineering and Industrial Aerodynamics **39**, 251–265 Publisher: Elsevier.

Frandsen, S., K. Thomsen, 1997: Change in fatigue and extreme loading when moving wind farms offshore. – Wind Engineering **21**, 197–214.

Garratt, J., 1990: The internal boundary layer – A review. – Boundary-Layer Meteorology **50**, 171–203 Publisher: Springer.

Garratt, J., 1994: The Atmospheric Boundary Layer – Cambridge University Press.

Garratt, J., B. Ryan, 1989: The structure of the stably stratified internal boundary layer in offshore flow over the sea. – Boundary-layer meteorology **47**, 17–40 Publisher: Springer.

Golbazi, M., C.L. Archer, 2019: Methods to estimate surface roughness length for offshore wind energy. – Advances in Meteorology **2019** Publisher: Hindawi.

Gottschall, J., B. Gribben, D. Stein, I. Würth, 2017: Floating lidar as an advanced offshore wind speed measurement technique: Current technology status and gap analysis in regard to full maturity. – Wiley Interdisciplinary Reviews: Energy and Environment **6**, e250 Publisher: Wiley Online Library.

Gottschall, J., E. Catalano, M. Dörenkämper, B. Witha, 2018: The NEWA ferry lidar experiment: measuring mesoscale winds in the Southern Baltic Sea. – Remote Sensing **10**, 1620 Publisher: Multidisciplinary Digital Publishing Institute.

Grayek, S., J. Staneva, J. Schulz-Stellenfleth, W. Petersen, E. Stanev, 2011: Use of FerryBox surface temperature and salinity measurements to improve model based state estimates for the German Bight. – J. Mar. Syst. **88**, 45–59, DOI: 10.1016/j.jmarsys.2011.02.020.

Gryning, S.E., J. Badger, A.N. Hahmann, E. Batchvarova, 2014: Current Status and Challenges in Wind Energy Assessment, 275–293 Springer New York, New York, NY, USA, DOI: 10.1007/978-1-4614-9221-4_13.

Hahmann, A.N., T. Sīle, B. Witha, N.N. Davis, M. Dörenkämper, Y. Ezber, E. García-Bustamante,

J.F. González-Rouco, J. Navarro, B.T. Olsen, S. Söderberg, 2020: The making of the new European wind atlas – part 1: Model sensitivity. – Geoscientific Model Development **13**, 5053–5078, DOI: 10.5194/gmd-13-5053-2020.

Hallgren, C., J. Arnqvist, S. Ivanell, H. Körnich, V. Vakkari, E. Sahlée, 2020: Looking for an offshore low-level jet champion among recent reanalyses: a tight race over the Baltic Sea. – Energies **13**, 3670 Publisher: Multidisciplinary Digital Publishing Institute.

Halvorsen-Weare, E.E., C. Gundegjerde, I.B. Halvorsen, L.M. Hvattum, L.M. Nonås, 2013: Vessel fleet analysis for maintenance operations at offshore wind farms. – Energy Procedia **35**, 167–176.

Hasager, C.B., D. Stein, M. Courtney, A. Peña, T. Mikkelsen, M. Stickland, A. Oldroyd, 2013: Hub height ocean winds over the North Sea observed by the NORSEWInD lidar array: measuring techniques, quality control and data management. – Remote Sensing **5**, 4280–4303 Publisher: Multidisciplinary Digital Publishing Institute.

Hasselmann, K.F., T.P. Barnett, E. Bouws, H. Carlson, D.E. Cartwright, K. Eake, J. Euring, A. Gicnapp, D. Hasselmann, P. Kruseman, others, 1973: Measurements of wind-wave growth and swell decay during the joint North Sea Wave project (JONSWAP). – Ergänzungsheft zur Deutschen Hydrographischen Zeitschrift, Reihe A

Haupt, S.E., B. Kosovic, W. Shaw, L.K. Berg, M. Churchfield, J. Cline, C. Draxl, B. Ennis, E. Koo, R. Kotamarthi, L. Mazzaro, J. Mirocha, P. Moriarty, D. Muñoz-Esparza, E. Quon, R.K. Rai, M. Robinson, G. Sever, 2019: On bridging a modeling scale gap: Mesoscale to microscale coupling for wind energy. – Bulletin of the American Meteorological Society **100**, 2533–2550, DOI: 10.1175/BAMS-D-18-0033.1.

He, Y.C., J.Y. Fu, Z.R. Shu, P.W. Chan, J.R. Wu, Q.S. Li, 2019: A comparison of micrometeorological methods for marine roughness estimation at a coastal area. – Journal of Wind Engineering and Industrial Aerodynamics **195**, 104010.

Hersbach, H., B. Bell, P. Berrisford, S. Hirahara, A. Horányi, J. Muñoz-Sabater, J. Nicolas, C. Peubey, R. Radu, D. Schepers, others, 2020: The ERA5 global reanalysis. – Quarterly Journal of the Royal Meteorological Society **146**, 1999–2049.

Howard, T., M. Palmer, G. Guentchev, J. Krijnen, 2019: Exploratory sea level projections for the uk to 2300. Technical Report SC150009, Environment Agency: Bristol, UK.

Høyer, J.L., I. Karagali, 2016: Sea surface temperature climate data record for the North Sea and Baltic Sea. – Journal of Climate **29**, 2529–2541.

Jensen, N.O., 1983: A note on wind generator interaction. Technical Report M-2411, RISOE, Roskilde, Denmark.

Jiang, Q., Q. Wang, 2021: Characteristics and scaling of the stable marine internal boundary layer. – Journal of Geophysical Research: Atmospheres **126**, e2021JD035510.

Jiang, Q., Q. Wang, S. Wang, S. Gaberšek, 2020: Turbulence adjustment and scaling in an offshore convective internal boundary layer: A casper case study. – Journal of the Atmospheric Sciences **77**, 1661–1681.

Jørgensen, H.E., M. Nielsen, R.J. Barthelmie, N.G. Mortensen, 2005: Modelling offshore wind resources and wind conditions. – In: Roskilde, Denmark: Risø National Laboratory, Kopenhagen.

Justus, C., A. Mikhail, 1976: Height variation of wind speed and wind distributions statistics. – Geophysical Research Letters **3**, 261–264 Publisher: Wiley Online Library.

Kalverla, P.C., J.B. Duncan Jr, G.J. Steeneveld, A.A. Holtslag, 2019: Low-level jets over the North Sea based on ERA5 and observations: together they do better. – Wind Energy Science **4**, 193–209 Publisher: Copernicus GmbH.

Katsaros, K.B., A. Fiúza, F. Sousa, V. Amann, 1983: Sea surface temperature patterns and air-sea fluxes in the German Bight during MARSEN 1979, phase 1. – Journal of Geophysical Research: Oceans **88**, 9871–9882.

Kawai, Y., A. Wada, 2007: Diurnal sea surface temperature variation and its impact on the atmosphere and ocean: A review. – Journal of Oceanography **63**, 721–744.

Kühn, M., J. Schneemann, 2017: Analyse der Abschattungsverluste und Nachlaufturbulenzcharakteristika großer Offshore-Windparks durch Vergleich von Alpha Ventus und Riffgat, GW Wakes: Abschlussbericht des Verbund-Forschungsprojekts: Laufzeit: 01.08.2011–30.09.2016; RAVE, Research at Alpha Ventus, eine Forschungsinitiative des Bundesumweltministeriums – Teilprojekt A durchgeführt im Rahmen von RAVE". Technical report, ForWind – Center for Wind Energy Research, Oldenburg, Germany, DOI: 10.2314/GBV:886719402.

Lampert, A., B.B. Jimenez, G. Gross, D. Wulff, T. Kenull, 2015: One year observations of the wind distribution and low-level jet occurrence at braunschweig, North German plain. – Wind Energy, DOI: 10.1002/we.1951.

Lampert, A., K. Bärfuss, A. Platis, S. Siedersleben, B. Djath, B. Cañadillas, R. Hunger, R. Hankers, M. Bitter, T. Feuerle, H. Schulz, T. Rausch, M. Angermann, A. Schwithal, J. Bange, J. Schulz-Stellenfleth, T. Neumann, S. Emeis, 2020: In situ airborne measurements of atmospheric and sea surface parameters related to offshore wind parks in the German Bight. – Earth Syst. Sci. Data **12**, 935–946.

Lange, B., S. Larsen, J. Højstrup, R. Barthelmie, 2004: Importance of thermal effects and sea surface roughness for offshore wind resource assessment. – Journal of wind engineering and industrial aerodynamics **92**, 959–988 Publisher: Elsevier.

Lee, J.C.Y., J.K. Lundquist, 2017: Evaluation of the wind farm parameterization in the weather research and forecasting model (version 3.8.1) with meteorological and turbine power data. – Geoscientific Model Development **10**, 4229–4244, DOI: 10.5194/gmd-10-4229-2017.

Lee, Y.H., K.D. Ahn, Y.H. Lee, 2016: Parametrization of the tidal effect for use in the Noah land-surface model: Development and validation. – Boundary-Layer Meteorology **161**, 561–574.

Lee, J., F. Zhao, A. Dutton, B. Backwell, L. Qiao, S. Lim, A. Lathigaralead, W. Liang, 2020a: GLOBAL OFFSHORE WIND REPORT 2020. Technical report, Global Wind Energy Council (GWEC), URL: https://gwec.net/global-offshore-wind-report-2020/.

Lee, Y.H., K.D. Ahn, Y.H. Lee, H. Eom, 2020b: Implementation of tidal parameterization in the weather research and forecasting (WRF) model. – Terrestrial, Atmospheric & Oceanic Sciences **31**.

Lehner, S., J. Horstmann, W. Koch, W. Rosenthal, 1998: Mesoscale wind measurements using recalibrated ERS SAR images. – Journal of Geophysical Research: Oceans (1978–2012) **103**, 7847–7856.

Leiding, T., B. Tinz, L. Gates, G. Rosenhagen, K. Herklotz, C. Senet, O. Outzen, A. Lindenthal, T. Neumann, R. Frühman, others, 2012: Standardisierung und vergleichende Analyse der meteorologischen FINO-Messdaten (FINO123). Technical report, Final Report–FINOWind Research Project, Hamburg, Germany.

Li, J., J. Scinocca, M. Lazare, N. McFarlane, K. Von Salzen, L. Solheim, 2006: Ocean surface albedo and its impact

on radiation balance in climate models. – Journal of climate **19**, 6314–6333 Publisher: American Meteorological Society.

Li, X., S. Lehner, 2013: Observation of TerraSAR-X for studies on offshore wind turbine wake in near and far fields. – Selected Topics in Applied Earth Observations and Remote Sensing, IEEE Journal of **6**, 1757–1768, DOI: 10.1109/JSTARS.2013.2263577.

Lima, D.C., P.M. Soares, A. Semedo, R.M. Cardoso, 2018: A global view of coastal low-level wind jets using an ensemble of reanalyses. – Journal of Climate **31**, 1525–1546 Publisher: American Meteorological Society.

Mauz, M., A. Rautenberg, A. Platis, M. Cormier, J. Bange, 2019: First identification and quantification of detached-tipvortices behind a wind energy converter using fixed-wing unmanned aircraft system. – Wind Energ. Sci. **4**, 451–463.

Mauz, M., van B. Kesteren, W. Junkermann, K. zum Berge, M. Schön, A. Platis, J. Bange, 2020: Miniature high-frequency chilled-mirror hygrometer for atmospheric measurements aboard fixed wing UAS. – Meteorol. Z. **29**, 439–449, DOI: 10.1127/metz/2020/1026.

Micallef, D., T. Sant, 2018: Rotor aerodynamics in sheared inflow: An analysis of out-of-plane bending moments. – J. Phys.: Conf. Ser. **1037**, 022027, DOI: 10.1088/1742-6596/1037/2/022027.

Miller, S., B. Keim, R. Talbot, H. Mao, 2003: Sea breeze: Structure, forecasting, and impacts. – Reviews of geophysics **41** Publisher: Wiley Online Library.

Mulhearn, P., 1981: On the formation of a stably stratified internal boundary-layer by advection of warm air over a cooler sea. – Boundary-Layer Meteorology **21**, 247–254 Publisher: Springer.

Nygaard, N.G., A.C. Newcombe, 2018: Wake behind an offshore wind farm observed with dual-Doppler radars. – In: Journal of Physics: Conference Series, volume 1037, 072008. IOP Publishing Issue: 7.

O'Carroll, A.G., E.M. Armstrong, H.M. Beggs, M. Bouali, K.S. Casey, G.K. Corlett, P. Dash, C.J. Donlon, C.L. Gentemann, J.L. Høyer, others, 2019: Observational needs of sea surface temperature. – Frontiers in Marine Science **6**, 420.

Openwind, 2020: Openwind user manual. Version 1.9.

Peña, A., C. Bay Hasager, J. Lange, 2013: Remote sensing for wind energy. Technical Report E-Report 0029(EN), DTU Wind Energy.

Platis, A., S. Siedersleben, J. Bange, A. Lampert, K. Bärfuss, R. Hankers, B. Cañadillas, R. Foreman, J. Schulz-Stellenfleth, B. Djath, T. Neumann, S. Emeis, 2018: First in situ evidence of wakes in the far field behind offshore wind farms. – Scientific Reports **8**, 2163.

Platis, A., J. Bange, K. Bärfuss, B. Cañadillas, M. Hundhausen, B. Djath, A. Lampert, J. Schulz-Stellenfleth, S. Siedersleben, T. Neumann, S. Emeis, 2020: Long-range modifications of the wind field by offshore wind parks – results of the project WIPAFF. – Meteorologische Zeitschrift (Contributions to Atmospheric Sciences) **29**, 355–376.

Platis, A., M. Hundhausen, M. Mauz, S. Siedersleben, A. Lampert, K. Bärfuss, B. Djath, J. Schulz-Stellenfleth, B. Canadillas, T. Neumann, S. Emeis, 2021: Evaluation of a simple analytical model for offshore wind farm wake recovery by in situ data and Weather Research and Forecasting simulations. Wind Energy **24**, 212–228.

Platis, A., M. Hundhausen, A. Lampert, S. Emeis, J. Bange, 2022: The Role of Atmospheric Stability and Turbulence in Offshore Wind-Farm Wakes in the German Bight. Boundary-Layer Meteorology **182**, 441–469.

Porté-Agel, F., M. Bastankhah, S. Shamsoddin, 2020: Wind-turbine and wind-farm flows: a review. – Boundary-Layer Meteorology **174**, 1–59 Publisher: Springer.

Pryor, S., R. Barthelmie, 1998: Analysis of the effect of the coastal discontinuity on near-surface flow. – In: Annales Geophysicae, volume 16, 882–888. Springer Issue: 7.

Rautenberg, A., J. Allgeier, S. Jung, J. Bange, 2019a: Calibration procedure and accuracy of wind and turbulence measurements with five-hole probes on fixed-wing unmanned aircraft in the atmospheric boundary layer and wind turbine wakes. – Atmosphere **10**, 124.

Rautenberg, A., M. Schön, zum K. Berge, M. Mauz, P. Manz, A. Platis, van B. Kesteren, I. Suomi, S.T. Kral, J. Bange, 2019b: The Multi-Purpose Airborne Sensor Carrier MASC-3 for Wind and Turbulence Measurements in the Atmospheric Boundary Layer. – Sensors **19**, 2292, DOI: 10.3390/s19102292. Publisher: MDPI AG.

Rott, A., J. Schneemann, F. Theuer, J.J. Trujillo Quintero, M. Kühn, 2022: Alignment of scanning lidars in offshore wind farms. – Wind Energ. Sci. **7**, 283–297, DOI: 10.5194/wes-7-283-2022.

Rybchuk, A., M. Optis, J.K. Lundquist, M. Rossol, W. Musial, 2021: A twenty-year analysis of winds in california for offshore wind energy production using WRF v4.1.2. – Geoscientific Model Development Discussions **2021**, 1–41, DOI: 10.5194/gmd-2021-50.

Schmidt, J., L. Vollmer, M. Dörenkämper, 2020: flappy version 0.4.1. https://gitlab.cc-asp.fraunhofer.de/iwes-cfsd/windsite-assessment/flappy Accessed: 2020-11-09.

Schneemann, J., J. Hieronimus, S. Jacobsen, S. Lehner, M. Kühn, 2015: Offshore wind farm flow measured by complementary remote sensing techniques: radar satellite TerraSAR-X and lidar windscanners. – J. Phys.: Conf. Ser. **625**, 012015, DOI: 10.1088/1742-6596/625/1/012015.

Schneemann, J., A. Rott, M. Dörenkämper, G. Steinfeld, M. Kühn, 2020: Cluster wakes impact on a far-distant offshore wind farm's power. – Wind Energy Science **5**, 29–49, DOI: 10.5194/wes-5-29-2020.

Schneemann, J., F. Theuer, A. Rott, M. Dörenkämper, M. Kühn, 2021: Offshore wind farm global blockage measured with scanning lidar. – Wind Energy Science **6**, 521–538, DOI: 10.5194/wes-6-521-2021.

Schulz-Stellenfleth, J., S. Foerderreuther, J. Horstmann, J. Staneva, 2021: Optimisation of Parameters in a German Bight Circulation Model by 4DVAR Assimilation of Current and Water Level Observations. – Frontiers in Marine Science **8:648266**, 1–22, DOI: 10.3389/fmars.2021.648266.

Shimada, S., T. Ohsawa, T. Kogaki, G. Steinfeld, D. Heinemann, 2015: Effects of sea surface temperature accuracy on offshore wind resource assessment using a mesoscale model. – Wind Energy **18**, 1839–1854 Publisher: Wiley Online Library.

Shimada, S., Y. Takeyama, T. Kogaki, T. Ohsawa, S. Nakamura, 2018: Investigation of the fetch effect using onshore and offshore vertical LIDAR devices. – Remote Sensing **10**, 1408 Publisher: Multidisciplinary Digital Publishing Institute.

Shimada, S., J.P. Goit, T. Ohsawa, T. Kogaki, S. Nakamura, 2020: Coastal wind measurements using a single scanning LiDAR. – Remote Sensing **12**, 1347 Publisher: Multidisciplinary Digital Publishing Institute.

Siedersleben, S., A. Platis, J. Lundquist, A. Lampert, K. Bärfuss, B. Cañadillas, B. Djath, J. Schulz-Stellenfleth, J. Bange, T. Neumann, S. Emeis, 2018a: Evaluation of a wind farm parametrization for mesoscale atmospheric flow models with aircraft measurements. – Meteorologische Zeitschrift **27**, 401–415.

Siedersleben, S.K., J.K. Lundquist, A. Platis, J. Bange, K. Bärfuss, A. Lampert, B. Cañadillas, T. Neumann,

S. Emeis, 2018b: Micrometeorological impacts of offshore wind farms as seen in observations and simulations. – Environmental Research Letters **13**, 124012 Publisher: IOP Publishing.

Simon, E., M. Courtney, 2016: A Comparison of sector-scan and dual Doppler wind measurements at Høvsøre Test Station–one lidar or two. Technical Report E-0112 (EN), DTU Wind Energy, Roskilde, Denmark.

Simpson, J., 1994: Sea breeze and local wind – Cambridge University Press, Cambridge (UK), 239.

Sinnett, G., F. Feddersen, 2018: The competing effects of breaking waves on surfzone heat fluxes: Albedo versus wave heating. – Journal of Geophysical Research: Oceans **123**, 7172–7184 Publisher: Wiley Online Library.

Skamarock, W.C., J.B. Klemp, J. Dudhia, D.O. Gill, D.M. Barker, W. Wang, J.G. Powers, 2008: A description of the Advanced Research WRF version 3. NCAR Technical note-475+ STR. Publisher: Citeseer.

Skamarock, W.C., J.B. Klemp, J. Dudhia, D.O. Gill, Z. Liu, J. Berner, W. Wang, J.G. Powers, M.G. Duda, D.M. Barker, others, 2019: A description of the advanced research WRF model version 4. – National Center for Atmospheric Research: Boulder, CO, USA 145.

Skyllingstad, E.D., R.M. Samelson, L. Mahrt, P. Barbour, 2005: A numerical modeling study of warm offshore flow over cool water. – Monthly weather review **133**, 345–361.

Smedman, A., U. Högström, H. Bergström, 1996: Low level jets – a decisive factor for off-shore wind energy siting in the Baltic Sea. – Wind Engineering **20**, 137–147.

Smedman, A.S., 1991: Occurrence of roll circulations in a shallow boundary layer. – Boundary-Layer Meteorology **57**, 343–358 Publisher: Springer.

Smedman, A.S., M. Tjernström, U. Högström, 1993: Analysis of the turbulent structure of a marine low-level jet. – Boundary-Layer Meteorology **66**, 105–126.

Smedman, A.S., H. Bergström, U. Högström, 1995: Spectra, variances and length scales in a marine stable boundary layer dominated by a low level jet. – Boundary-Layer Meteorology **76**, 211–232.

Smedman, A.S., H. Bergström, B. Grisogono, 1997: Evolution of stable internal boundary layers over a cold sea. – Journal of Geophysical Research: Oceans **102**, 1091–1099.

SPD, Bündnis 90/Die Grünen, FDP, 2021: Mehr Fortschritt wagen, Bündnis für Freiheit, Gerechtigkeit und Nachhaltigkeit – Koalitionsvertrag zwischen SPD, Bündnis 90/Die Grünen und FDP. last visit: 27.01.2022.

Spyridonidou, S., D.G. Vagiona, 2020: Systematic Review of Site-Selection Processes in Onshore and Offshore Wind Energy Research. – Energies **13**, 5906 Publisher: Multidisciplinary Digital Publishing Institute.

Sterl, A., A.M. Bakker, van den H.W. Brink, R. Haarsma, A. Stepek, I.L. Wijnant, de R.C. Winter, 2015: Large-scale winds in the southern North Sea region: the wind part of the KNMI'14 climate change scenarios. – Environmental Research Letters **10**, 035004.

Stull, R.B., 1988: An Introduction to boundary layer meteorology – Kluwer Academic Publishers.

Svensson, N., E. Sahlée, H. Bergström, E. Nilsson, M. Badger, A. Rutgersson, 2017: A case study of offshore advection of boundary layer rolls over a stably stratified sea surface. – Advances in Meteorology **2017**.

Sweeney, J., J. Chagnon, S. Gray, 2014: A case study of sea breeze blocking regulated by sea surface temperature along the English south coast. – Atmospheric Chemistry and Physics **14**, 4409–4418 Publisher: Copernicus GmbH.

Taylor, P., 1969: On wind and shear stress profiles above a change in surface roughness. – Quarterly Journal of the Royal Meteorological Society **95**, 77–91 Publisher: Wiley Online Library.

Taylor, P.A., 1970: A model of airflow above changes in surface heat flux, temperature and roughness for neutral and unstable conditions. – Boundary-Layer Meteorology **1**, 18–39, DOI: 10.1007/BF00193902.

Theuer, F., van M.F. Dooren, von L. Bremen, M. Kühn, 2020: Minute-scale power forecast of offshore wind turbines using long-range single-Doppler lidar measurements. – Wind Energy Science **5**, 1449–1468, DOI: 10.5194/wes-5-1449-2020.

Trabucchi, D., J.J. Trujillo, J. Schneemann, M. Bitter, M. Kühn, 2014: Application of staring lidars to study the dynamics of wind turbine wakes. – Meteorologische Zeitschrift **24**, 557–564, DOI: 10.1127/metz/2014/0610.

Türk, M., S. Emeis, 2010: The dependence of offshore turbulence intensity on wind speed. – Journal of Wind Engineering and Industrial Aerodynamics **98**, 466–471.

Troen, I., E.L. Petersen, 1989: European Wind Atlas. Technical report, Risoe National Laboratory, Roskilde, Denmark.

Valldecabres, L., N. Nygaard, L. Von Bremen, M. Kühn, 2018: Very short-term probabilistic forecasting of wind power based on dual-Doppler radar measurements in the North Sea. – In: Journal of Physics: Conference Series, volume 1037, 052010. IOP Publishing Issue: 5, DOI: 10.1088/1742-6596/1037/5/052010.

Van Der Laan, M., A. Pena, P. Volker, K.S. Hansen, N.N. Sørensen, S. Ott, C.B. Hasager, 2017: Challenges in simulating coastal effects on an offshore wind farm. – In: Journal of Physics: Conference Series, volume 854, 012046. IOP Publishing Issue: 1.

Vasiljević, N., G. Lea, M. Courtney, J.P. Cariou, J. Mann, T. Mikkelsen, 2016: Long-range WindScanner system. – Remote Sensing **8**, 896, DOI: 10.3390/rs8110896. Publisher: Multidisciplinary Digital Publishing Institute.

Viana, R.D., J.A. Lorenzzetti, J.T. Carvalho, F. Nunziata, 2020: Estimating energy dissipation rate from breaking waves using polarimetric SAR images. – Sensors **20**, 6540.

Vickers, D., L. Mahrt, J. Sun, T. Crawford, 2001: Structure of offshore flow. – Monthly Weather Review **129**, 1251–1258.

Volker, P.J.H., J. Badger, A.N. Hahmann, S. Ott, 2015: The explicit wake parametrisation v1.0: a wind farm parametrisation in the mesoscale model WRF. – Geoscientific Model Development **8**, 3715–3731, DOI: 10.5194/gmd-8-3715-2015.

Vollmer, L., G. Steinfeld, M. Kühn, 2017: Transient LES of an offshore wind turbine. – Wind Energy Science **2**, 603–614, DOI: 10.5194/wes-2-603-2017.

Wagner, D., G. Steinfeld, B. Witha, H. Wurps, J. Reuder, 2019: Low Level Jets over the Southern North Sea. – Meteorologische Zeitschrift **28**, 389–415 Publisher: Science Publishers, DOI: 10.1127/metz/2019/0948.

Wahl, T., I.D. Haigh, P.L. Woodworth, F. Albrecht, D. Dillingh, J. Jensen, R.J. Nicholls, R. Weisse, G. Wöppelmann, 2013: Observed mean sea level changes around the North Sea coastline from 1800 to present. – Earth-Science Reviews **124**, 51–67.

Wahle, K., J. Staneva, W. Koch, L. Fenoglio-Marc, H. Ho-Hagemann, E.V. Stanev, 2017: An atmosphere–wave regional coupled model: improving predictions of wave heights and surface winds in the southern North Sea. – Ocean Science **13**, 289–301.

Wang, Q., D.P. Alappattu, S. Billingsley, B. Blomquist, R.J. Burkholder, A.J. Christman, E.D. Creegan, T. De Paolo, D.P. Eleuterio, H.J.S. Fernando, others, 2018: Casper: Coupled air–sea processes and electromagnetic ducting research. – Bulletin of the American Meteorological Society **99**, 1449–1471.

Wever, N., 2012: Quantifying trends in surface roughness and the effect on surface wind speed observations. – Journal of Geophysical Research: Atmospheres **117** Publisher: Wiley Online Library.

Wildmann, N., M. Mauz, J. Bange, 2013: Two fast temperature sensors for probing of the atmospheric boundary layer using small remotely piloted aircraft (RPA). – Atmospheric Measurement Techniques **6**, 2101–2113, DOI: 10.5194/amt-6-2101-2013. Publisher: Copernicus GmbH.

Wildmann, N., F. Kaufmann, J. Bange, 2014a: An inverse-modelling approach for frequency response correction of capacitive humidity sensors in abl research with small remotely piloted aircraft (rpa). – Atmos. Meas. Tech. **7**, 3059–3069.

Wildmann, N., S. Ravi, J. Bange, 2014b: Towards higher accuracy and better frequency response with standard multi-hole probes in turbulence measurement with remotely piloted aircraft (RPA). – Atmos. Meas. Tech. **7**, 1027–1041.

WindEurope, 2020: The European offshore wind industry – key trends and statistics 2019. Technical report, 40 pages, Wind Europe.

Woollings, T., D. Barriopedro, J. Methven, S.W. Son, O. Martius, B. Harvey, J. Sillmann, A.R. Lupo, S. Seneviratne, 2018: Blocking and its response to climate change. – Current Climate Change Reports **4**, 287–300.

Yang, Z., A. Calderer, S. He, F. Sotiropoulos, R. Krishnamurthy, L.S. Leo, H.J.S. Fernando, C.M. Hocut, L. Shen, 2019: Measurement-based numerical study of the effects of realistic land topography and stratification on the coastal marine atmospheric surface layer. – Boundary-Layer Meteorology **171**, 289–314.

Zhang, X., J.W. Bao, B. Chen, E.D. Grell, 2018: A three-dimensional scale-adaptive turbulent kinetic energy scheme in the WRF-ARW model. – Monthly Weather Review **146**, 2023–2045, DOI: 10.1175/MWR-D-17-0356.1.

Ziemann, A., A. Galvez Arboleda, A. Lampert, 2020: Comparison of wind lidar data and numerical simulations of the low-level jet at a grassland site. – Energies **13**, 6264.